

SURVEY AND SUMMARY

A critical analysis of methods used to investigate the cellular uptake and subcellular localization of RNA therapeutics

Kirsten Deprey, Nefeli Batistatou and Joshua A. Kritzer¹*

Department of Chemistry, Tufts University, 62 Talbot Ave, Medford, MA 02155, USA

Received May 25, 2020; Revised June 17, 2020; Editorial Decision June 23, 2020; Accepted June 24, 2020

ABSTRACT

RNA therapeutics are a promising strategy to treat genetic diseases caused by the overexpression or aberrant splicing of a specific protein. The field has seen major strides in the clinical efficacy of this class of molecules, largely due to chemical modifications and delivery strategies that improve nuclease resistance and enhance cell penetration. However, a major obstacle in the development of RNA therapeutics continues to be the imprecise, difficult, and often problematic nature of most methods used to measure cell penetration. Here, we review these methods and clearly distinguish between those that measure total cellular uptake of RNA therapeutics, which includes both productive and non-productive uptake, and those that measure cytosolic/nuclear penetration, which represents only productive uptake. We critically analyze the benefits and drawbacks of each method. Finally, we use key examples to illustrate how, despite rigorous experimentation and proper controls, our understanding of the mechanism of gymnotic uptake of RNA therapeutics remains limited by the methods commonly used to analyze RNA delivery.

INTRODUCTION

RNA therapeutics are an emerging drug class currently being applied to the treatment of genetic diseases caused by an overexpressed or aberrantly spliced protein. RNA therapeutics are short, chemically modified nucleic acids whose base sequences target disease-associated genetic material in the cell with high selectivity. The term ‘RNA therapeutics’ includes antisense oligonucleotides (ASOs), small interfering RNAs (siRNAs), microRNAs, and RNA ap-

tamers. ASOs and siRNAs, first described in 1978 and 1998 (1,2), respectively, are currently the most widely applied in drug development. Single-stranded ASOs modify protein expression by binding to the target mRNA, and then, depending on chemical modifications and their targeted location on the mRNA, either cause RNase H-mediated degradation, correct aberrant splicing, or block ribosomal assembly (3,4). siRNAs are larger, double-stranded oligonucleotides that cause mRNA degradation through an RNA-induced silencing complex (RISC)-mediated pathway (5). Because they could in principle target any mRNA, RNA therapeutics have a vast potential, especially to treat genetic diseases that are currently untreatable by conventional medicine. Decades of work have made the design and synthesis of ASOs and siRNAs relatively straightforward (6,7). Additionally, in contrast to small molecules and other drug modalities, the pharmacokinetic properties of RNA therapeutics can, for the most part, be optimized independently from their target affinity, which is largely determined by their base sequence (8). Justifiably, drug development using RNA therapeutics has seen an exponential rise in investment during the last two decades (9).

There are currently many RNA therapeutics in use and in clinical trials. As of May 2020, a total of seven ASO drugs have been approved for use in humans: fomivirsen for cytomegalovirus retinitis (10), mipomersen for familial hypercholesterolemia (11), nusinersen for spinal muscular atrophy (12), eteplirsen and golodirsen for Duchenne muscular dystrophy (13,14), inotersen for hereditary transthyretin amyloidosis (15) and volanesorsen for familial chylomicronemia (16). Of these, four were approved by the United States Food and Drug Administration (US FDA), and two were discontinued due to a decrease in the number of treatable patients (fomivirsen) or competing treatments (mipomersen) (17). Two siRNA drugs have been approved by the US FDA, patisiran for hereditary transthyretin amyloidosis (18) and givosiran for acute hepatic porphyria (19).

*To whom correspondence should be addressed. Tel: +1 617 627 0451; Email: joshua.kritzer@tufts.edu

Many additional ASOs and siRNAs are currently undergoing clinical trials (17,20). In a recent and well-publicized ‘N-of-one’ trial, a child with a rare neurodegenerative genetic disorder called Batten’s disease was treated with a personalized ASO drug called milasen. Milasen was designed with the same chemical scaffold as nusinersen, but with a base sequence that would correct the specific splicing error caused by the child’s unique genetic mutation (21). Within a year, milasen was produced, tested, approved, and administered to the young patient. These and other success stories provide a glimpse into the vast potential of RNA therapeutics to treat genetic disorders, and potentially other acute and chronic diseases, which are difficult or impossible to treat with traditional small molecule therapies.

Despite their promise, development of RNA therapeutics is fraught with many of the same difficulties as small molecule drug development, along with many difficulties unique to this modality. RNA therapeutics have failed clinical trials for a large variety of reasons, including toxicity, off-target tissue sequestration, inactivity once delivered to the target tissue, and even failure to reach the clinical endpoint despite causing alterations in protein expression (22–24). Some of these failures are due to incomplete understanding of the underlying biology and the poor predictive power of animal models, which are unfortunate features of all modern drug development. However, other clinical failures can be attributed to poor tissue targeting and cell penetration, and these remain major obstacles in the field. Over the last 15 years, a large effort has been undertaken in both academic and industrial labs to gain a mechanistic understanding of how RNA therapeutics are internalized by cells. In this review, we discuss experimental methods that have been used to measure cell penetration by RNA therapeutics, with the goal of distinguishing methods that measure total cellular uptake from methods that can more specifically measure penetration to the cytosol or nucleus. This distinction is important for a critical analysis of methods used to monitor how RNA therapeutics enter cells, and for illustrating how those methods currently limit our understanding of the underlying mechanisms.

DISCUSSION

Chemical modifications and delivery strategies for RNA therapeutics

Cellular delivery of RNA therapeutics faces two main issues: oligonucleotides are susceptible to degradation by nucleases, and their cellular uptake can be inefficient (8). For ASOs and siRNAs, the primary means of addressing both of these issues has been through chemical modifications. RNA therapeutics can employ a great diversity of chemical modifications on their phosphates, sugars and nucleobases—this area has been reviewed (25), so here we will summarize the most widely used modifications. Phosphorothioate (PS) backbones and 2′-O-methyl (2′-OMe) ribose sugars are commonly used to increase nuclease resistance and promote cellular uptake (26–28). Importantly, ASOs that are fully modified with PS- and 2′-O-methyl groups are not able to recruit RNase H1 and cleave the target mRNA. To balance favorable pharmacokinetic properties with mRNA-degradation activity, ‘gap-

mers’ were introduced (29). Gapmers have a middle region of PS-deoxynucleotides, allowing for RNase H1 recruitment, flanked by 2′-modified PS-nucleotides on either side. Additional 2′ modifications including 2′-O-methoxyethyl (2′-MOE) are used to increase the hydrophobicity of the therapeutic, which enhances its binding to the membrane receptors and facilitates cellular uptake (30). Conformational restriction, which can improve binding affinity and selectivity for the mRNA target, can be introduced by linking the 2′-oxygen and 4′-carbon of the ribose, giving rise to a locked nucleic acid (LNA) (31). In a separate approach to backbone modification, cationic groups such as guanidinium can be added to the backbone. Guanidinium and other cationic groups are known to interact with the anionic cell surface and facilitate cellular uptake (32), and this modification has shown some promise in promoting cellular uptake for ASOs (33). For siRNAs, which are larger and require separate sense and antisense strands, a large variety of backbone and sugar modifications have been evaluated. Commonly, siRNAs incorporate specific patterns of 2′-OMe, 2′-fluoro (2′-F) and phosphorothioate modifications at the 5′ and 3′ ends of both the sense and antisense strands. While the impact of specific modification patterns on the activity of siRNAs is still being investigated, these modifications together enhance target binding affinity and nuclease stability, while still allowing for association with the RISC complex (8).

Incorporating the chemical modifications described above can render ASOs and siRNAs highly resistant to degradation by nucleases, and they can also improve apparent cell penetration. However, gymnosis (the process by which RNA therapeutics are taken up by the cell, unfacilitated by other chemical or physical means of drug delivery) (34) remains highly inefficient. One way of bypassing inefficient gymnosis is to employ physical or chemical delivery strategies (35). Physical strategies for drug delivery include microinjection, electroporation and compression (36–38). They require the application of a physical needle or probe, electric field, or high pressure in order to physically disrupt the plasma membrane. Though these techniques ensure efficient delivery of the therapeutic to the cytosol with little loss to other compartments, they are painstaking and laborious, and can be damaging to the cell. Further, most physical delivery strategies are not immediately applicable to *in vivo* studies or clinical administration. Chemical strategies for delivery, by contrast, have been applied in animals and even in humans. The most commonly used chemical strategy *in vitro* is transfection using cationic lipids such as lipofectamine (39,40), but applications *in vivo* are limited due to high potential for toxicity (41). Formulation of RNA therapeutics into liposomes or lipid nanoparticles, containing both cationic and neutral lipids to promote delivery while avoiding toxicity, can promote delivery across the plasma membrane (42). This strategy is used clinically—the siRNA drug patisiran is delivered using lipid nanoparticles (18). Direct chemical conjugation of RNA therapeutics to lipids such as cholesterol or to cell-penetrating peptides also promotes cell penetration (43–45). Conjugation of RNA therapeutics to other chemical groups can further promote cell entry as well as tissue targeting (46). For example, ASOs conjugated to N-acetylgalactosamine bind specifically to

the asialoglycoprotein receptor, which is abundant in liver tissue, and are selectively taken up by hepatocytes *in vitro* and *in vivo* (47). Chemical delivery strategies have great advantages, but each strategy has strengths and weaknesses. Overall, the main drawbacks are fast clearance, which requires administration of high doses, and accumulation of toxic material, which can be dose-limiting.

Investigation of the molecular mechanisms of gymnosis and various chemical delivery strategies has intensified in recent years (see below). Often, RNA therapeutics are observed to be taken up by cells, but still do not exert a change in mRNA levels or protein expression. This phenomenon has been termed ‘non-productive uptake’, while uptake that leads to a phenotypic effect has been termed ‘productive uptake’ (48). Mechanistically, gymnosis and most chemical delivery strategies rely on endocytosis for cellular uptake (Figure 1). Most of the material taken up by endocytosis remains trapped in endosomal vesicles. This trapped material is inactive since it cannot interact with its cellular target in the cytosol or nucleus, and either remains trapped in endosomes or gets delivered to the lysosome, where it is degraded. Collectively, this is the material that can be said to have undergone non-productive uptake, because it remains associated with the cell but does not lead to any cellular activity. In a poorly understood process, RNA therapeutics can escape into the cytosol from late endosomes. This material can access the cellular target in the cytosol or nucleus, and it can be said to have undergone productive uptake.

While assays that measure the activity of an RNA therapeutic can imply the relative degree of productive uptake, assays that measure cell penetration more directly do not measure productive versus non-productive uptake. Rather, they measure either **total cellular uptake** or **cytosolic/nuclear penetration**. **Total cellular uptake** is the total amount of RNA therapeutic that remains associated with the cell following treatment. Importantly, this includes material bound at the cell surface and material trapped in endosomal compartments. **Cytosolic/nuclear penetration** refers to the fraction of RNA therapeutic that has successfully accessed the cytosolic/nuclear compartment. While RNA therapeutics can be active in the cytosol or in the nucleus (49), and some studies have shown selective localization in one compartment over the other (50–52), for the sake of this discussion we will group these compartments together as ‘cytosolic/nuclear’ to distinguish them from compartments that prevent activity, such as endosomes and lysosomes. Ultimately, cytosolic/nuclear material is what leads to the observation of productive uptake, while the difference between total cellular uptake and cytosolic/nuclear penetration constitutes non-productive uptake (Figure 1).

Methods to measure functional activity of RNA therapeutics

In the studies that first described antisense technology, a 13-mer DNA oligonucleotide was applied to chick embryo fibroblasts infected with the Rous sarcoma virus to inhibit viral replication (1). The incorporation of synthetic radioactive nucleotides was used as a measure of the virus’ reverse transcriptase activity (1). Cells treated with the antisense oligonucleotide showed a decrease in reverse transcriptase

activity, which indirectly suggested uptake of the exogenous antisense oligonucleotide.

While the methodology for monitoring relevant phenotypes has advanced, the most common ways to measure the productive uptake of RNA therapeutics still involve readouts of functional activity. Today, reverse-transcriptase polymerase chain reaction (RT-PCR) is often used to quantitate target mRNA knockdown or splicing (Figure 2A). After treatment with the RNA therapeutic, cells or tissues are lysed and mRNA is extracted from the lysates. Primers corresponding to the target mRNA transcript are added, and RT-PCR is performed to quantitate the extent of mRNA knockdown or splicing. RT-PCR is quantitative and high throughput, and since it measures activity of RNA therapeutics that have presumably penetrated to the cytosol or nucleus, endosomally trapped material does not contribute to its signal. In parallel, knockdown of the target protein is typically monitored by Western blot (Figure 2B).

A hybridization-based approach can also be used to detect degradation of target mRNA. Fluorescence *in situ* hybridization (FISH) uses a dye-labeled oligonucleotide probe to detect changes in mRNA levels (Figure 2A) (53–56). The dye-labeled probe is complementary to the target mRNA which allows it to be used to monitor knockdown. After treatment with RNA therapeutic, the cells are fixed and treated with the dye-labeled probe. Unhybridized probe is removed during wash steps, and the location and intensity of hybridized probe is analyzed by fluorescence microscopy. This allows direct and quantitative measurement of mRNA levels, allowing one to measure the activities of different RNA therapeutics and thus indirectly to measure their degree of cytosolic/nuclear penetration. Unlike RT-PCR, the FISH signal is directly proportional to the abundance of the target mRNA because the readout is non-amplified. However, the lack of amplification means FISH is not as sensitive as RT-PCR. Additionally, wash steps must be extensive to avoid high background from excess, unhybridized probe.

Some investigations do not involve a specific endogenous target. In these cases, an exogenously introduced reporter protein can be used to measure activity (Figure 2B). The most common reporters are luciferase and green fluorescent protein, whose expression can be measured through straightforward spectroscopic techniques (57–60). Such reporters can be used for RNA therapeutics that induce degradation of their target mRNA, but also for RNA therapeutics that modulate mRNA splicing. For these ‘splice-switching’ assays, the RNA therapeutic is incubated with a cell line that expresses either reporter protein, in which the mRNA transcript is interrupted by a large intron (61,62). If the oligonucleotide can access the nucleus and reaches the pre-mRNA transcript, it will redirect splicing and remove the interruption, resulting in a functional full-length protein. For experiments using cultured cells, luciferase or GFP expression is commonly measured with a plate reader or flow cytometer (61,62).

While measuring mRNA and protein levels is more direct, activity can also be quantitated by measuring phenotypic changes (Figure 2C). In cell culture, these phenotypic assays may take the form of cell viability experiments after treatment with an antisense oligonucleotide that knocks down a critical cellular protein. For example, PS- and 2’-

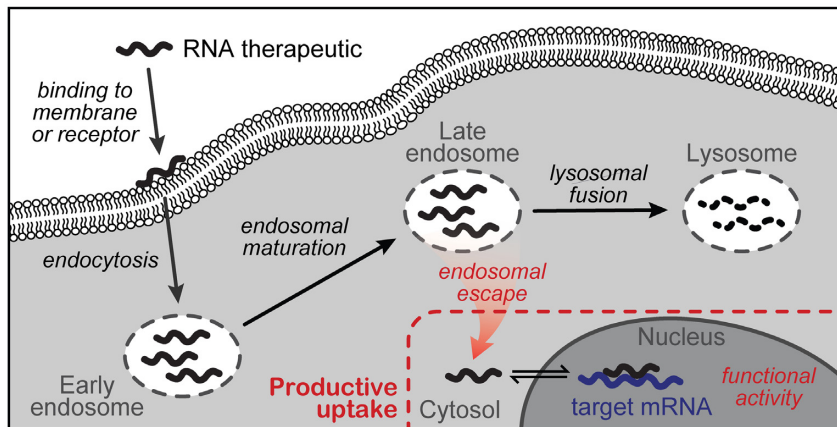


Figure 1. Productive uptake of RNA therapeutics. The RNA therapeutic binds the plasma membrane or a membrane receptor and is taken up by the cell via endocytosis. It is initially trapped in early endosomes, which mature into late endosomes. The RNA therapeutic can be trafficked to the lysosome to be degraded, and the total amount of material that is trapped in endosomes and degraded is referred to as ‘non-productive uptake.’ Alternatively, the RNA therapeutic can escape from the endosome into the cytosol, from which it can access the nucleus and exert its therapeutic effect (functional activity). ‘Productive uptake’ therefore includes only material that accessed the cytosol and/or nucleus. Methods for measuring cell penetration of RNA therapeutics can either measure total cellular uptake, which includes all material associated with the cell including material trapped in endosomes, or cytosolic/nuclear penetration, which includes only material that contributes to functional activity.

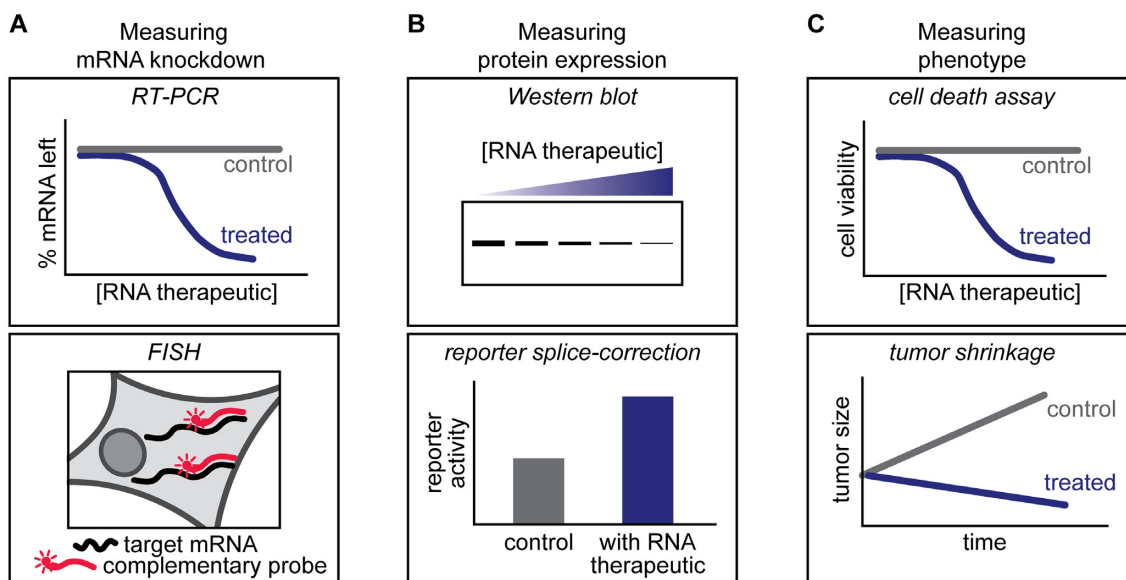


Figure 2. Assays that measure functional activity of RNA therapeutics. After application of the RNA therapeutic, functional activity can be measured in many different ways. Some common examples include (A) detection of mRNA knockdown by RT-PCR or fluorescence in situ hybridization (FISH), (B) detection of altered protein expression through Western blot or splice correction of a reporter protein and (C) detection of phenotypic changes by cell death or tumor shrinkage.

MOE-modified gapmer oligonucleotides targeted to Bcl-2 and Bcl-xL mRNAs were incubated with human glioma cells in culture, and one assay that was used to compare the relative cytosolic/nuclear penetration of these oligonucleotides was a crystal violet assay for cell viability (63). However, viability assays can be problematic since RNA therapeutics can be toxic at high concentrations (depending on chemical modifications and the delivery strategy, 0.2–10 μ M or higher) (64,65). Sequence-specific cytotoxicity of modified oligonucleotides has also been observed (66). Thus, it can be difficult to deconvolute on-target cell-killing activity from less specific toxicity due to cell per-

meabilization or changes in global gene expression (67). *In vivo*, if the target is involved in cancer, the phenotypic assay can involve reduction in tumor growth or inhibition of tumor formation. For example, an LNA-containing oligonucleotide targeting TGF- β 2 was analyzed for efficacy through a reduction in tumor growth of lung metastases (68). Overall, such phenotypic assays are indirect measures of cytosolic/nuclear penetration, because they are influenced by many other factors.

Of course, functional activity assays are critical for drug development, as the goal for any RNA therapeutic is to have a biological effect. Activity assays integrate all aspects of

a molecule's efficacy, from target access to target binding to subsequent translation, in a fairly straightforward and high-throughput manner. Further, the readout from activity assays does not require a covalent label for detection, so these assays can compare productive uptake independent from the impact of a chemical label.

Although these studies are undeniably crucial in the pipeline of an RNA therapeutic, they also inherently miss a great deal of information on cellular uptake, subcellular trafficking, and endosomal escape. For instance, the activity assays discussed in this section are amplificative, so the signal is not directly proportional to the extent of uptake. Amplified assays provide for greater sensitivity, but do not allow for quantitative comparisons. Thus, they are not ideal for structure-activity relationship studies that seek to understand the effects of different chemical modifications. In addition, activity-based assays integrate a large number of processes, any of which could impact the final readout. If an RNA therapeutic does not have the expected biological effect, it could be due to lack of total uptake, lack of endosomal escape, trafficking to the lysosome, sequestration within subcellular structures, nonspecific interactions with proteins or protein complexes, aggregation, degradation, low target affinity, high degree of secondary structure, failure to recruit ribonucleases or block the spliceosome, or many other factors. Ideally, one would subject the RNA therapeutics of interest, plus controls, to many assays that each measure one of these diverse factors. However, because cytosolic/nuclear penetration is such an important roadblock to activity for RNA therapeutics, failure in an activity-based assay is often ascribed to poor productive uptake (poor cytosolic/nuclear penetration, Figure 1) (69). One can control for some aspects of internalization using an experiment in which RNA therapeutics and controls are introduced into the cell via different delivery strategies. However, this experiment only controls for a limited part of the internalization process and does not directly address most of the other factors listed above. Ultimately, activity assays are most informative in conjunction with assays that measure total cellular uptake and assays that directly measure cytosolic/nuclear penetration.

Methods to measure total cellular uptake

Understanding how to promote productive uptake of RNA therapeutics is critical to the development of effective therapeutics, yet the methods available to measure cell penetration have distinct weaknesses. The ideal method would be quantitative, high-throughput, label-free, and able to distinguish unambiguously among subcellular compartments. In this section, we discuss methods that measure total cellular uptake; methods that measure cytosolic/nuclear penetration are discussed in the next section. Methods commonly applied to measure the total cellular uptake of peptide drugs were recently reviewed (70,71). Here, we focus on an overlapping set of methods commonly applied to RNA therapeutics.

Measuring total cellular uptake of labeled RNA therapeutics. In early studies, oligonucleotides radiolabeled with ³⁵S phosphorothioates were incubated with cells, and to-

tal radioactivity was measured after extensive washing (39,72,73). This method has also been applied *in vivo* to measure accumulation of a ³H- or ³⁵S-labeled oligonucleotide in specific tissues (74–76). Radioactive labeling and detection methods are no longer widely used in early stage preclinical research due to high cost of materials and safety concerns. Radioactivity-based assays have been largely replaced in favor of other detection methods, such as fluorescence (77).

The most commonly used method for measuring total cellular uptake is tracking fluorescence of dye-labeled RNA therapeutics. For these experiments, dye-labeled oligonucleotides are incubated with cells in culture or administered *in vivo* with subsequent tissue harvesting. Total cellular uptake is most often measured by flow cytometry (Figure 3A) or fluorescence microscopy (Figure 3B) (44,78–82). Flow cytometry is quantitative and high-throughput, but the signal of internalized dye-labeled molecules is indistinguishable from that of dye-labeled molecules bound to the outside of the plasma membrane or trapped in endosomes. Live-cell fluorescence microscopy is lower-throughput than flow cytometry, but microscopy is better able to distinguish subcellular localization. However, it is difficult even with confocal fluorescence microscopy to determine definitively the extent to which a dye-labeled molecule is cytosolic or endosomal without advanced techniques. Further, each of these methods requires labeling of the RNA therapeutic of interest with a bulky and hydrophobic dye. In some cases, addition of the dye can influence the extent of uptake and subcellular trafficking by altering interactions with the plasma membrane and embedded proteins, and effects of dye labeling have been observed for cell-penetrant peptides as well (83–85). Another liability of these commonly used assays is that degradation of the molecule releases the free dye, and thus could result in a false-positive signal (67,86). Despite these caveats, flow cytometry and fluorescence microscopy are still two of the most widely used methods to measure total cellular uptake of RNA therapeutics.

Other, more advanced fluorescence-based techniques have been implemented to address some of the drawbacks of flow cytometry and fluorescence microscopy (Figure 3C) (87,88). Fluorescence lifetime imaging microscopy (FLIM) can measure the total cellular uptake and stability of RNA therapeutics in cultured cells (52,89–93). The fluorescence lifetime of a fluorophore can be altered when it is in close proximity to another fluorophore or when it is in different chemical environments, such as packaged in a delivery vector, trapped in an endosome, or free in the cytosol (91,94,95). FLIM has been used for the detection of porphyrin-oligonucleotide conjugates, where the porphyrin aided in both delivery and detection of the oligonucleotide (90). In principle, FLIM can distinguish endosomally trapped and cytosolic material, but in practice FLIM signal is altered in subtle ways by the type of dye used and the chemical environment of each subcellular structure. As a result, it remains difficult to quantitate localization to subcellular structures using FLIM, and thus FLIM is best characterized as a method for quantitating total cellular uptake.

Another alternative that uses dye-labeled oligonucleotides is capillary electrophoresis with laser-induced fluorescence (CE-LIF, Figure 3D), which has been used to

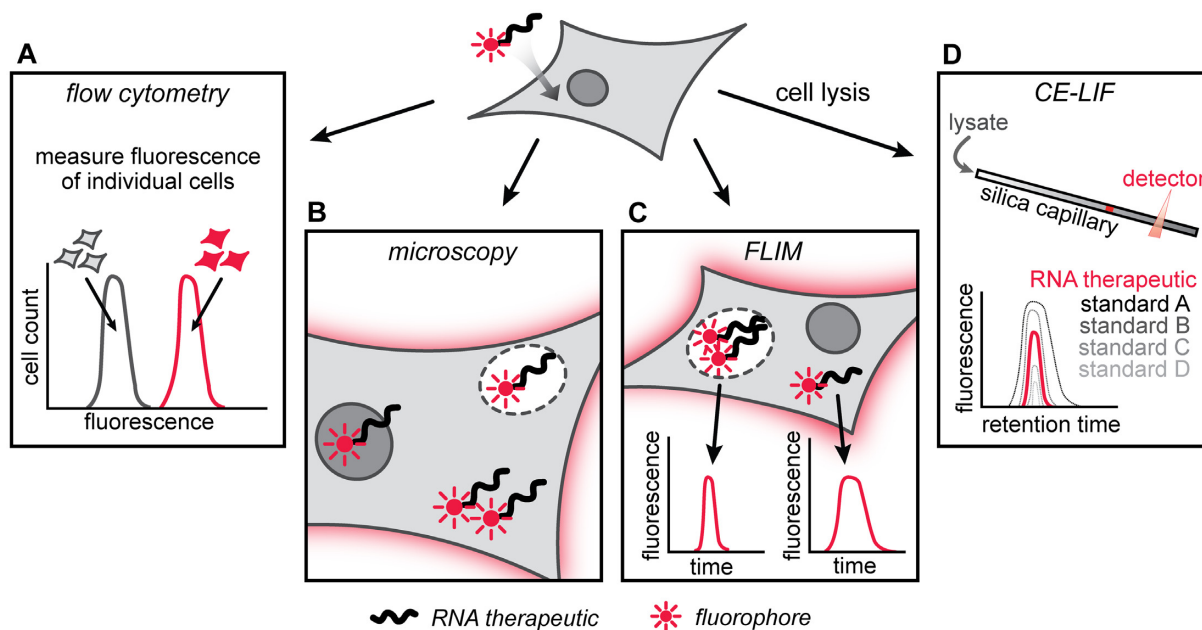


Figure 3. Assays that measure total cellular uptake of dye-labeled RNA therapeutics. Cells in culture can be treated with a dye-labeled RNA therapeutic and the fluorescence within live cells can then be measured by (A) flow cytometry, (B) confocal fluorescence microscopy or (C) fluorescence lifetime imaging microscopy (FLIM). (D) Fluorescence can also be measured in cell lysates by capillary electrophoresis with laser-induced fluorescence (CE-LIF).

quantitate the concentration of dye-labeled nucleic acids in solution (96). In a related experiment, CE-LIF was also used to measure concentration of endogenous target mRNA in plasma and human cells through the use of a complementary dye-labeled DNA probe (97–99). CE-LIF has also been applied to quantitation of RNA therapeutics delivered by scrape-loading (100,101), liposome encapsulation (102,103) and peptide conjugation (104). In a typical CE-LIF experiment, the cells are lysed and the soluble fraction is injected onto a capillary column for separation by capillary electrophoresis. The dye-labeled oligonucleotide is detected with a laser excitation beam at the appropriate wavelength, and the concentration of internalized molecule is calculated from a calibration curve of standards of known concentration spiked into untreated cell lysate (100,101). This method is very sensitive and requires very small (nL–pL) sample volumes (102). CE-LIF measures total cellular uptake because cell lysis results in the mixing and re-equilibration of membrane-bound, endosomal, and cytosolic/nuclear material prior to analysis. It also carries the same caveats as flow cytometry and fluorescence microscopy with respect to the dye potentially altering penetration properties.

Measuring total cellular uptake of label-free RNA therapeutics. A handful of assays that measure total cellular uptake eliminate the need for a label entirely. Immunofluorescence, traditionally used to detect proteins, and also has recently been adapted for the detection of RNA therapeutics *in vitro* using anti-oligonucleotide antibodies (Figure 4A) (44,105–107). Cells treated with PS-oligonucleotides are washed, fixed, permeabilized, blocked, treated with an anti-oligonucleotide primary antibody, and finally treated with a dye-labeled secondary antibody. The fluorescence

from the secondary antibody is detected by fluorescence microscopy, and fluorescence can be quantitated to measure the relative amount of internalized oligonucleotide. Additional co-localization studies with membrane proteins involved in endocytosis can aid in the study of subcellular localization (44,105,107). Immunofluorescence assays can be performed using unlabeled oligonucleotides, and the use of antibodies for detection renders this method highly specific. However, immunofluorescence must be performed on fixed and permeabilized cells in order to deliver the antibodies to the interior of the cell. Oligonucleotides and other biomolecules have been shown to redistribute throughout the cell as a result of fixation, leading to false-positive artifacts (33,51,86,108,109). Finally, even with careful colocalization studies, it can be difficult to deconvolute cytosolic versus endosomal material in a definitive manner.

Another label-free method for measuring total cellular uptake of RNA therapeutics is in-cell nuclear magnetic resonance (NMR, Figure 4B). Unique NMR chemical shifts for artificial nucleic acids can be observed in cell lysates and live cells. (110–113) The Trantirek group was the first to perform in-cell NMR to detect exogenously applied oligonucleotides, delivered by physical injection of live *Xenopus laevis* oocytes (111). The oligonucleotides were doubly-labeled with ^{13}C and ^{15}N . The spectra obtained from live cells were compared to those obtained from the lysates of treated cells and to those obtained *in vitro*. These NMR-based experiments have since been applied to live human cells (113), and have been adapted to quantify the uptake of RNA therapeutics. In this adaptation, the molecules were delivered to the cell via electroporation or transfection, and the ^1H spectra were recorded (114,115). To enhance sensitivity, the Petzold group performed $^1\text{H},^{31}\text{P}$ cross-polarization dynamic nuclear polarization NMR on frozen cells electropo-

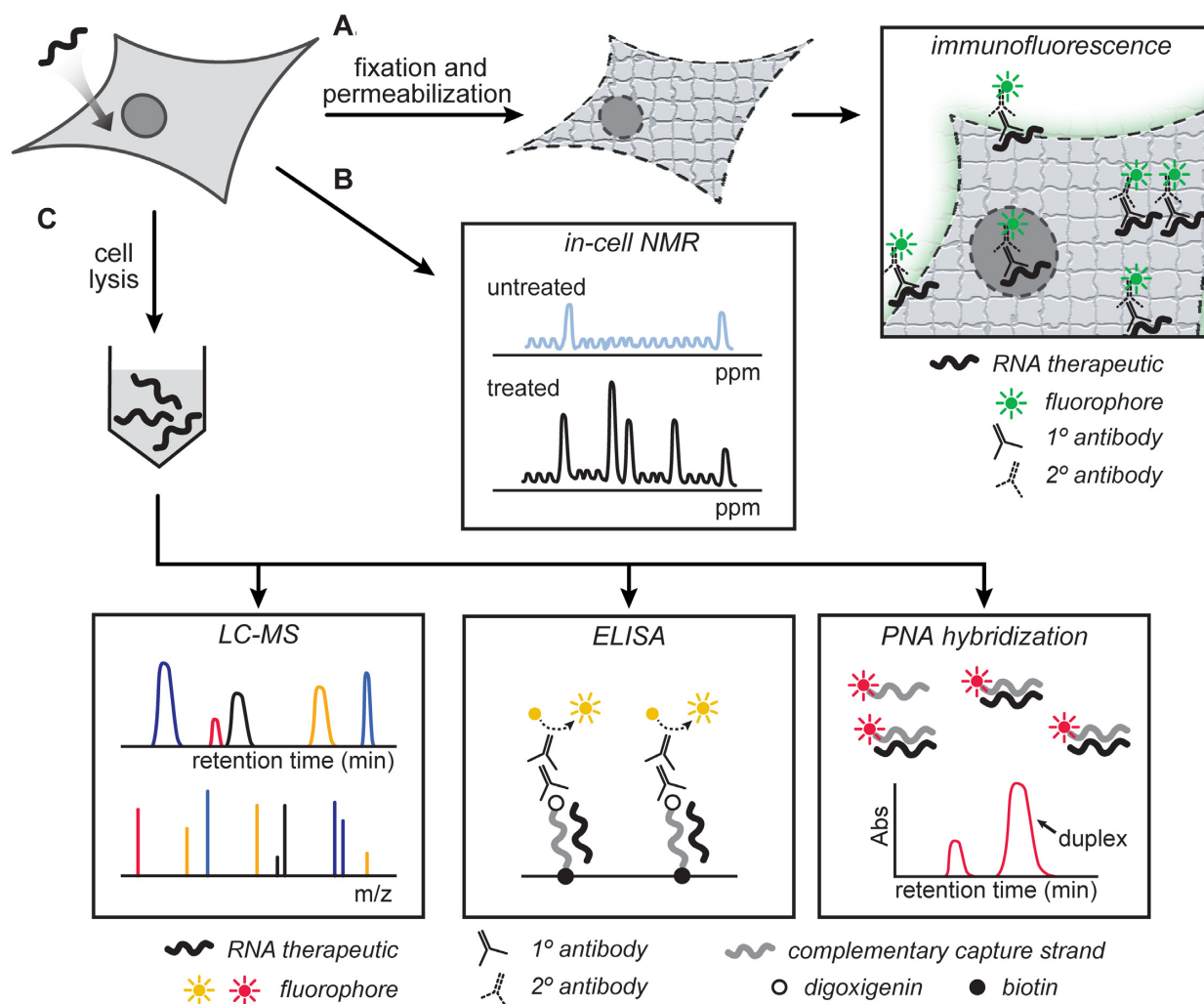


Figure 4. Assays that measure total cellular uptake of label-free RNA therapeutics. First, cells or tissues are treated with unlabeled RNA therapeutic. (A) For immunofluorescence detection of unlabeled RNA therapeutics, cells or tissues are fixed, permeabilized, and incubated with dye-labeled antibodies that selectively recognize the RNA therapeutic. (B) Using advanced NMR techniques, delivered RNA therapeutics can be measured in intact cells by quantitating peak volumes from the NMR spectra of ^{31}P or other nuclei. (C) After homogenization and lysis of cells or tissues, the concentration of unlabeled RNA therapeutic in the cell lysate can be measured by enzyme-linked immunosorbent assay (ELISA), a peptide nucleic acid (PNA) hybridization assay, or by liquid chromatography–mass spectrometry (LC–MS).

rated with a PS-modified gapmer oligonucleotide (115). The peak volumes of the ^{31}P NMR spectra were used to estimate the concentration of the oligonucleotide. No detectable signal was observed in cells that underwent free uptake of the oligonucleotide (115). This may be due to the micromolar concentrations required for detection by NMR using moderate acquisition times. Other limitations of NMR-based quantitation include the requirement for careful construction of calibration curves, and the interference in NMR spectra from other molecules in cells and complex lysates.

While NMR-based quantitation suffers from a lack of sensitivity, mass spectrometry methods are notable for their excellent sensitivity. Mass spectrometry methods are becoming more and more common for measuring the total cellular uptake of RNA therapeutics, both in cultured cells and *ex vivo* (42,107,116–119). Cells or tissues are homogenized and lysed, and the cleared lysates are analyzed by liquid

chromatography and mass spectrometry (LC–MS, Figure 4C) (42,107,116–119). LC–MS can be made quantitative by calibrating with standards of known concentration spiked into cell lysate. With appropriate calibration, this method can have both high sensitivity and excellent quantitation.

Other label-free assays take advantage of the selective nature of hybridization by using a labeled complementary strand for isolation and quantification of the RNA therapeutic. One example is the adaptation of the enzyme-linked immunosorbent assay (ELISA) to measure total cellular uptake and tissue distribution of antisense oligonucleotides (Figure 4C) (50,120–127). In most of these examples, a cell lysate is incubated with a biotinylated oligonucleotide complementary to the RNA therapeutic. Then the hybridized duplex is captured on avidin-coated magnetic beads. The biotinylated complementary oligonucleotide is also labeled at the opposite end with digoxigenin, to allow for detection of the immobilized duplexes with an alkaline

phosphatase-conjugated anti-digoxigenin antibody. Alkaline phosphatase activity is used as a measure of the relative amount of original oligonucleotide that was pulled down. ELISA-based detection methods are very sensitive and can detect concentrations as low as picomolar in complex matrices including tissue lysates (122,125,127). However, with the enhanced sensitivity comes the drawback that this assay is amplificative, which complicates quantitative comparisons of total cellular uptake. ELISA, as with Western blotting, involves many steps with a high number of manipulations, which reduces throughput and can lead to artifacts. Additionally, antibodies must be carefully selected to ensure that they are specific and robust to manipulation.

Another assay that relies on hybridization is the peptide-nucleic acid (PNA) hybridization assay (Figure 4C). PNA hybridization assays are widely used to measure the total cellular uptake of modified oligonucleotides and siRNAs in cultured cells, as well as in plasma samples and in tissues *ex vivo* (81,128–135). For this assay, cells or tissues that have been exposed to the RNA therapeutic are homogenized and lysed. The soluble lysates are incubated with a complementary, dye-labeled PNA, which hybridizes to the RNA therapeutic. HPLC retention time is used to distinguish duplex PNA-RNA from unhybridized PNA, and peak volume can be used to quantitate the concentration of duplexed PNA using a calibration curve of PNA duplexes of known concentration spiked into the cell lysate (128). PNA hybridization assays are highly specific, quantitative, and label-free with respect to the RNA therapeutic. However, tissue homogenization and cell lysis allow the PNA probes to hybridize with RNA therapeutic that was once endosomally trapped or membrane-bound. Therefore, while this assay has many advantages, it only measures total cellular uptake and cannot distinguish between cytosolic and endosomal compartments.

All of the assays described in this section measure total cellular uptake, which is the total amount of material associated with the cell or tissue (Figure 1). This includes material that is trapped in endosomes or lysosomes, and material that remains bound to the cell surface after wash steps. For most methods, the need to fix or lyse cells results in mixing and equilibration of components from different compartments. Confocal microscopy is performed on live cells, and therefore does not require cells to be fixed and permeabilized. With careful co-localization, confocal microscopy is sometimes able to distinguish endosomal and lysosomal material from cytosolic material. However, this distinction requires extensive and time-consuming analysis, and signal from endolysosomal compartments cannot entirely be eliminated.

Overall, there is a great deal of evidence that RNA therapeutics, especially when delivered via gymnosin, accumulate in endosomal compartments with a relatively small proportion escaping to the cytosol. Endosomally trapped RNA therapeutics are unable to reach their intracellular target, leading to potential overestimation of productive uptake if conclusions are drawn solely from assays that measure total cellular uptake. Such conclusions are to be avoided, as this may be a primary reason for poor success when using *in vitro* experiments to predict *in vivo* potency.

Methods to measure cytosolic/nuclear penetration

Assays that measure material that has localized to the cytosol and/or nucleus, without interference from material stuck at the plasma membrane or in endosomal compartments, are crucial for the development of RNA therapeutics. In this section, we discuss methods that can selectively quantitate cytosolic and nuclear material. Many of the assays described in the previous section on total cellular uptake can offer information about subcellular localization through the use of subcellular fractionation (50,72,75,107,136). Ultracentrifugation of cell lysates allows for separation of cellular structures, which in principle allows for the separation of membrane-bound, endosomal, cytosolic and nuclear-localized material (137). However, in practice subcellular fractionation is technically challenging and low-throughput, involving painstaking manipulations of the lysate samples. Cross-contamination between subcellular compartments must be rigorously tested for and controlled against. Even with careful controls, material can re-equilibrate during lysis prior to ultracentrifugation, further reducing confidence that this method can faithfully distinguish material that resided in different compartments in the live, intact cell (137). Several alternatives can more reliably eliminate endosomally trapped material from interfering with measurements of cytosolic/nuclear penetration of RNA therapeutics.

As described above, conventional fluorescence microscopy techniques such as immunofluorescence and confocal fluorescence microscopy are largely qualitative and cannot easily distinguish between cytosolic and endosomal material. Immunofluorescence and confocal microscopy work well in principle to distinguish endosomal material from cytosolic/nuclear material, but in practice endosomal and cytosolic/nuclear material can be confounding. These assays require extensive co-localization analysis to provide confidence in any conclusions about subcellular localization.

Fluorescence correlation spectroscopy assays. More advanced fluorescence techniques are capable of better quantitation of the amount of dye-labeled molecule within the cell, and they can also better distinguish subcellular compartments. A key example is fluorescence correlation spectroscopy (FCS) (138), which has been applied to investigate the concentrations of RNA therapeutics in live cells (Figure 5A) (52,53,91,93). In FCS, the diffusion of a dye-labeled molecule is tracked within a small (femtoliter) focal volume by measuring fluctuations in fluorescence intensity of molecules entering and exiting the focal volume. The absolute number of molecules present within the defined focal volume can be calculated using a Poisson distribution (139). Cytosolic material is distinguished from endosomal material through imaging analysis that identifies regions that do not include punctate signal, which represent endolysosomal vesicles (140). Focal volumes within these regions are chosen manually. The Mundigl group at Roche recently used FCS to calculate the absolute number of microinjected LNA-gapmer oligonucleotides required for target gene suppression (53). Scientists in the Brock group at Radboud University Medical Center also used FCS to measure the

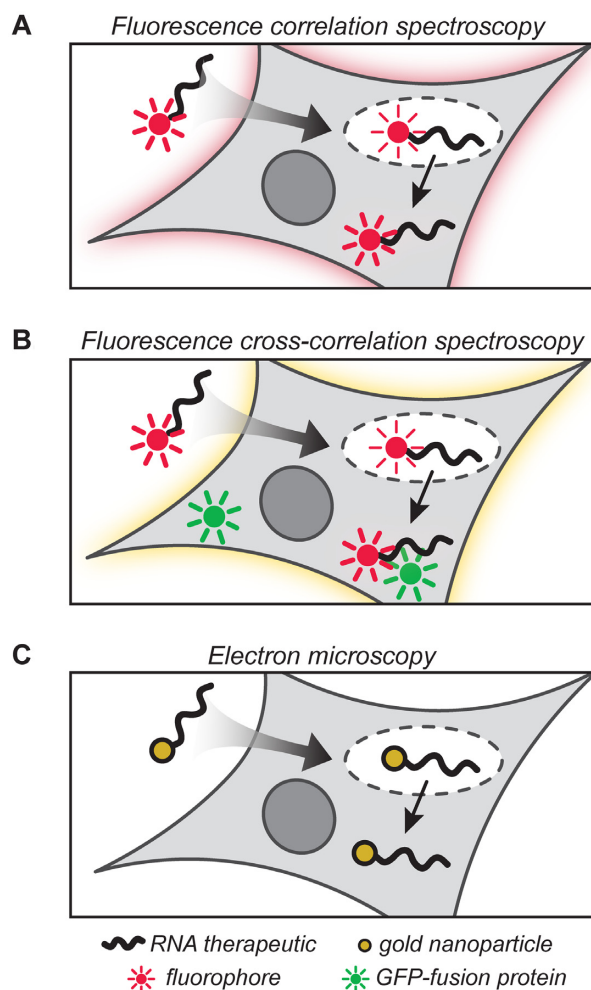


Figure 5. Assays that measure cytosolic/nuclear penetration of labeled RNA therapeutics. (A) Fluorescence correlation spectroscopy measures the diffusion of a small number of dye-labeled molecules through a defined cytosolic focal volume. (B) Fluorescence cross-correlation spectroscopy measures the diffusion of a small number of dye-labeled molecules through a defined cytosolic focal volume, tracked simultaneously with another fluorescent molecule or protein of interest. (C) Electron microscopy detects gold nanoparticle-labeled molecules, and can distinguish material in the cytosol from material in various endosomal compartments.

nuclear concentration of a splice-switching oligonucleotide delivered by polyplex formation with cell-penetrant peptides, correlating the concentration to the observed therapeutic effects in a cell culture model of myotonic dystrophy (93).

FCS was further adapted into a dual-color technique called fluorescence cross-correlation spectroscopy (FCCS) (Figure 5B) (141). FCCS involves the same principles as FCS but tracks two fluorescent dyes simultaneously. If the variations of intensity over time within a small focal volume align well in the two different color channels, then that observation is indicative that the two fluorophores are in close proximity to one another (141). The Schwille group used FCCS to analyze the incorporation of microinjected dye-labeled siRNAs into the RISC complex, visualized using an expressed Argonaute2-EGFP fusion in both the cytosol and nucleus (142). In another example, researchers in the

Wagner and Lamb groups at the University of Munich used FCCS to assess the cytosolic degradation of dual-labeled oligonucleotides through simultaneous tracking of both fluorophores of a FRET pair (52).

FCS and FCCS allow calculation of absolute concentration of a dye-labeled RNA therapeutic, as opposed to the relative fluorescence intensities obtained from simpler fluorescence microscopy techniques (143). Despite this and other advantages, FCS and FCCS are low-throughput, require specialized instrumentation, are limited to applications in cell culture, and require a fluorescent dye to be conjugated to the RNA of interest. Further, the process requires the user to manually select focal volumes to analyze within the cell, which may introduce some degree of subjectivity. These drawbacks may explain why, despite their sensitivity, their absolute quantitation, and their ability to interrogate exclusively cytosolic or nuclear material, FCS and FCCS have yet to be adopted by a larger number of groups interested in RNA therapeutics.

Electron microscopy assays with siRNA-gold. Gilleron et al used electron microscopy to measure the cellular amount of siRNA-gold after *in vitro* and *in vivo* delivery using lipid nanoparticles (144). Cells or tissues were administered siRNA which was covalently labeled with gold nanoparticles. At different timepoints, cells or tissues were washed, fixed, stained, and subjected to electron microscopy to detect the subcellular localization of the gold nanoparticles (Figure 5C) (144). Electron microscopy allows one to morphologically distinguish subcellular structures such as early endosomes, late endosomes, and lysosomes. The high resolution of this method enables clear measurement of the proportion of siRNA-gold in endosomal, cytosolic and nuclear compartments. However, this method is low throughput, requires fixation, and necessitates labeling of the siRNA with gold nanoparticles, and has not been widely adopted.

The available methods for measuring functional activity and total cellular uptake are far more numerous and far more accessible than the available methods for measuring cytosolic/nuclear penetration. New, more easily adopted methods that measure cytosolic/nuclear penetration of RNA therapeutics are thus critically needed. Existing methods that have been developed for peptide and protein delivery could readily be adapted for use with RNA therapeutics (70,71). For example, several assays measure a signal that depends on interaction between the exogenously applied molecule and a protein expressed in the cytosol/nucleus. These assays include split-protein complementation assays (145–147), glucocorticoid receptor transcriptional reporter assays (148,149), biotin ligase assays (150), and assays that involve enzyme-specific fluorogenic probes (151). Each of these assays comes with caveats of their own, which are discussed elsewhere (70,71), but they also offer valuable information about the cytosolic/nuclear penetration of exogenously applied molecules. With relatively straightforward adjustments, each of these assays could be directly applied to measuring the cytosolic/nuclear penetration of RNA therapeutics.

Another promising assay that relies on interactions with expressed proteins is the chloroalkane penetration assay (CAPA) (152–154). CAPA uses a HeLa cell line that sta-

bly expresses the engineered protein HaloTag to quantify the cytosolic penetration of molecules labeled with a small chloroalkane ligand (155). Cells are pulsed with the chloroalkane-labeled molecule, which covalently reacts with HaloTag upon reaching the cytosol. This covalent reaction blocks the active sites of the HaloTag protein. Cells are then chased with a chloroalkane-labeled dye, which reacts with open active sites. The total fluorescence from the dye, measured by flow cytometry, is inversely proportional to the concentration of cytosolic RNA therapeutic. CAPA signal excludes material stuck in endosomes or at the cell surface, and CAPA is non-amplified so the signal is a direct and quantitative measurement of the amount of material delivered. Our group originally developed CAPA to measure the cytosolic penetration of various cell-penetrating peptides, and others have adapted it for use with small molecules, peptidomimetics and cell-penetrant proteins (156–161). We are currently applying CAPA to diverse RNA therapeutics with different chemical modifications, in order to better understand factors that drive cytosolic/nuclear penetration.

Methodology limits our understanding of the molecular mechanisms of gymnosis

RNA therapeutics can be delivered to the cell using a variety of strategies, all of which may have different mechanisms, rates of uptake and degrees of cytosolic/nuclear penetration. Gymnosis refers to the cytosolic/nuclear penetration of nucleic acids without facilitation by physical disruption or chemical agents (34). The mechanisms of gymnosis are poorly understood, yet gymnotic uptake is central to the drug development strategy of many clinically important RNA therapeutics (34,162,163). It is critical to recognize that the methods used to analyze uptake directly affect the conclusions that can, and cannot, be drawn. Thus, in this section, we will address what is known about the mechanisms of gymnosis of RNA therapeutics, highlighting the limitations of the methods used.

It is generally accepted that RNA therapeutics are internalized by the cell through endocytosis after associating with proteins on the cell membrane (69,163–165). After the initial uptake, the RNA therapeutic is trapped inside the early endosome. During endosome maturation, RNA therapeutics may escape these vesicles and subsequently exert their therapeutic effect in the nucleus or cytosol (Figure 1) (69,163,166,167). Endosomal escape is thought to be attributed to some degree of membrane deformation of the late endosome or a small degree of leakage from vesicle fusion processes (69,80,144,163,166,167).

The experiments required to understand the subcellular trafficking of RNA therapeutics are challenging, and their difficulty has limited progress in understanding the exact mechanisms of endosomal escape. Recently, some investigators have taken a genetics-based approach to implicate specific cellular proteins in gymnotic uptake and endosomal escape. Most commonly, specific genes were individually knocked down to identify proteins involved in gymnosis (166,168–170). Less commonly, specific genes involved in uptake of RNA therapeutics were also identified using siRNA knockdown screens with small libraries of siRNAs

targeting genes associated with vesicle trafficking (105). A list of specific proteins identified as important for gymnosis is included in Table 1. Typically, once the protein involved was implicated using knockdown, methods for quantitating total cellular uptake were used to more precisely define that protein's role in gymnotic uptake. However, as mentioned above, different assays have different limitations, which potentially limit the conclusions that can be drawn about the role of the implicated protein. Below, we highlight three illustrative examples of authors who rigorously implemented available assays and drew sound conclusions, but whose conclusions are inherently limited due to the nature of the assays.

Example 1. AP2M1 mediates productive uptake. In 2011, Koller *et al.* determined that the adaptor protein AP2M1 is crucial for the functional uptake of single-stranded RNA therapeutics into primary murine MHT cells. AP2M1 is an adaptor protein, involved in clathrin-mediated endocytosis, that is recruited to the membrane in a cargo-dependent manner. AP2M1 binds cytosolic-facing PI(4,5)-P₂ membrane lipids, clathrin, and additional accessory and adaptor proteins. It thus provides an indirect link between exogenous cargo interaction with the plasma membrane and clathrin polymerization required for clathrin-mediated endocytosis (171,172). Knockdown of AP2M1 decreased the total cellular uptake of a dye-labeled oligonucleotide by nearly 50%, and decreased functional activity by a similar degree. Uptake was measured by applying Cy3- and fluorescein-labeled oligonucleotides to MHT cells in culture and then analyzing using flow cytometry. Additionally, LC-MS was performed on the lysates of treated cells with standards of known concentration spiked into the lysates for quantitation. Further, immunofluorescence studies were performed on fixed cells using an anti-PS-oligonucleotide antibody. In parallel, RT-PCR and Western blot were used to monitor the knockdown of target mRNA and protein, respectively. Taken together, the data from these assays were used to conclude that AP2M1 is important for productive uptake.

While these data can firmly conclude that AP2M1 is involved in the earliest steps of gymnotic uptake (binding the cell surface and endocytosis, Figure 1), they cannot conclude anything about its role in later steps such as endosomal escape. Surprisingly, while both total cellular uptake and functional activity were reduced upon siRNA-mediated knockdown of AP2M1, only total cellular uptake was reduced upon siRNA-mediated knockdown of clathrin, while functional activity was unaffected. The reason for this discrepancy could not be addressed with the methods used. Specifically, flow cytometry and LC-MS can only measure total material associated with the cell, and cannot distinguish among membrane-bound, cytosolic and endosomal material. The discrepancy between total cellular uptake and functional activity observed after AP2M1 and clathrin were both knocked down could be explained by a role for AP2M1 in endosomal escape, and potentially a degree of independence between rate of clathrin-mediated endosomal uptake and rate of endosomal escape. However, given the indirect nature of functional activity assays, these hypotheses remain untested.

Table 1. Selected proteins shown to be important for gymnosis of RNA therapeutics, their known roles in gymnosis, and the methods used (other than functional assays) to verify their importance for gymnosis. PS: phosphorothioate, MOE: 2' *O*-methoxyethyl, LNA: locked nucleic acid

Protein(s)	Implicated step in gymnosis (Figure 1)	RNA therapeutic	Methods used	Reference
Stabilin-1 and Stabilin-2	Endocytosis	Cy3- and ¹²⁵ I- labeled PS-MOE gapmer ASOs	Fluorescence microscopy, immunohistochemistry, radioactivity	(169)
Adaptor protein (AP2M1)	Endocytosis	Cy3- and fluorescein-labeled PS-MOE gapmer ASOs	Flow cytometry, immunofluorescence, mass spectrometry	(105)
Caprin-1	Not identified, hypothesized role in endocytosis	Cy3-labeled peptide-PNA conjugates	Fluorescence microscopy	(173)
Systemic RNA interference deficient-1 transmembrane family 2 (SIDT2)	Not identified, hypothesized role in endocytosis	Alexa568-labeled PO-2' <i>O</i> -methyl ASOs, dsRNA	Fluorescence microscopy	(168)
Annexin A2	Endosomal maturation	Cy3-labeled PS-MOE gapmer ASOs	Subcellular fractionation, flow cytometry, co-localization microscopy after fixation	(166)
Epidermal growth factor receptor (EGFR)	Endocytosis, Endosomal maturation	Cy3-labeled gapmer ASOs with PS-MOE, PS-F, and PS-cEt modifications	Flow cytometry, co-localization microscopy after fixation	(170)
Protein Kinase C-alpha (PKCα)	Endosomal maturation	Cy5-labeled PS-LNA gapmer ASOs	flow cytometry	(174)
ESCRT-1 proteins: tumor susceptibility gene 101 (TSG101) and VPS28	Endocytosis Endosomal maturation	PS-DNA, cEt and MOE-ASOs, and PS-F, MOE-ASO	luciferase knockdown, viability	(175)
Coat protein complex II (COPII) and associated proteins: SEC31a, Sar1, STX5	Endosomal escape	Cy3-labeled PS-MOE gapmer ASOs, and Cy3-labeled 5-10-5 PS-LNA gapmer ASOs	Flow cytometry, co-localization microscopy after fixation	(80)
Mannose-6-phosphate receptor (M6PR) and associated tethering protein, GCC2	Endosomal escape	Cy3-labeled PS-MOE gapmer ASOs	Flow cytometry, microscopy after fixation and co-localization	(176)
Rab5c	Endosomal maturation	PS-MOE gapmer ASO ¹²⁵ I-labeled PS-MOE gapmer ASO	Radioactivity	(177)
Early endosomal antigen 1 (EEA1)	Endosomal maturation	PS-MOE gapmer ASO ¹²⁵ I-labeled PS-MOE gapmer ASO	Radioactivity	(177)
Rab7	Endosomal maturation, Lysosome biogenesis and fusion, Endosomal escape	PS-MOE gapmer ASO ¹²⁵ I-labeled PS-MOE gapmer ASO	Radioactivity	(177)
Lysobisphosphatidic acid (LBPA)	Endosomal escape	Cy3-labeled PS-MOE gapmer ASOs	Flow cytometry, co-localization microscopy after fixation	(167,177)
Alix	Endosomal escape	Cy3-labeled PS-MOE gapmer ASOs	Flow cytometry, co-localization microscopy after fixation	(167,177)

Example 2. Stabilin-1 and stabilin-2 promote productive uptake. In 2016, the Harris and Seth groups found that, in addition to previously reported scavenger receptors, stabilin-1 and stabilin-2 are implicated in the internalization of chemically modified oligonucleotides (169). The stabilin-oligonucleotide binding event triggered uptake by clathrin-mediated endocytosis, resulting in functional antisense activity in cells and tissues. HEK-293 cell lines stably expressing stabilin-1 or stabilin-2 had both a higher degree of internalization and increased antisense activity compared to a HEK-293 cell line stably expressing a blank vector. Total cellular uptake of oligonucleotide in stabilin-expressing cells was reduced in the presence of known stabilin ligands, which indicates a process that can be competitively saturated. These findings were consistent with direct binding of

the oligonucleotide to stabilins, followed by endocytic internalization of the receptor and the oligonucleotide.

Multiple assays were used in parallel to elucidate the roles of stabilin proteins in the internalization of PS-oligonucleotides. Uptake was measured by: fluorescence microscopy of a Cy3-labeled oligonucleotide in cell culture using co-localization with lysotracker, immunohistochemistry using an anti-PS-oligonucleotide antibody in tissue samples comparing wild type and stabilin-2-knockout mice, and total radioactivity of ¹²⁵I-labeled oligonucleotide in cell culture. Additionally, expression of target mRNA *in vitro* and *ex vivo* was measured by RT-PCR to assess the activity of the applied oligonucleotide. Cells and tissues expressing stabilin-1 and stabilin-2 had reduced signals by microscopy, immunohistochemistry, and total radioactivity of

cell lysates, and a larger extent of target mRNA knock-down was observed in stabilin-positive cells as compared to stabilin-negative cells.

Stabilin-1 and stabilin-2 are clearly involved in the internalization of PS-oligonucleotides, starting with direct binding at the cell surface. However, the roles of stabilins once PS-oligonucleotides are internalized into endosomes remain unknown because the methods could only measure total cellular uptake and not localization into different compartments. Further, some discrepancies were found when comparing data obtained from the three different methods, which emphasize the need for careful interpretation of data on cellular uptake. For instance, the cells expressing stabilin-2 demonstrated higher total cellular uptake of an ^{125}I -labeled RNA therapeutic than cells expressing stabilin-1, measured by total radioactivity. However, stabilin-2-expressing cells showed lower mRNA degradation efficiency than the stabilin-1-expressing cells. Despite the application of several uptake assays and functional assays, it remains unclear whether these discrepancies are due to binding affinity, efficiency of total cellular uptake, efficiency of endosomal escape, trafficking in the cytosol or nucleus, or any other factors downstream from the initial internalization event. The authors acknowledged that confocal fluorescence microscopy could not unambiguously detect from Cy3-labeled RNA therapeutic in the nucleus due to the high signal of oligonucleotides in endosomes and lysosomes (169). This common finding highlights that fluorescence microscopy can provide some degree of distinction among dye-labeled RNA therapeutics at the plasma membrane, in endosomes, in lysosomes, in the cytosol, and in the nucleus. But even in conjunction with careful co-localization studies, it can be very challenging to use confocal fluorescence microscopy to quantitate cytosolic and nuclear material, particularly if the efficiency of endosomal escape is low. Importantly, while the activity data provide the ultimate measure of potency, performing RT-PCR on the target mRNA does not provide precise information about endosomal escape efficiency because it involves several steps of signal amplification. Further, functional assays cannot elucidate which specific steps in the internalization pathway are different between two molecules with different potencies. As such, this example highlights that multiple assays that measure total cellular uptake, even combined with functional assays, cannot conclude definitively how key proteins are involved in the endosomal trafficking and escape of RNA therapeutics.

Example 3. COPII vesicles facilitate endosomal escape. Recently, scientists in the Crooke group at Ionis Pharmaceuticals identified coat protein complex II (COPII)-containing vesicles and associated tethering protein STX5 as facilitators of endosomal escape of single-stranded PS-oligonucleotides (80). COPII vesicles are normally involved in ER-Golgi transport processes, but they were observed to localize to late endosomes containing PS-oligonucleotides and facilitate their endosomal release. siRNA knockdown of COPII reduced antisense activity, yet had no effect on the total cellular uptake of PS-oligonucleotides and no effect on trafficking of molecules from the early to late endosome. Knockdown of STX5 also resulted in reduced anti-

sense activity and reduced co-localization of COPII and the applied oligonucleotide. It was concluded that STX5 is recruited to late endosomes containing PS-oligonucleotides, binds to PS-oligonucleotides, and in turn recruits COPII vesicles to late endosomes, which together enhance endosomal escape of the applied RNA therapeutic.

The conclusions of this study were drawn from a combination of several methods. Activity of the RNA therapeutic was measured with RT-PCR of the target mRNA and Western blots of the target protein. Total cellular uptake was measured with flow cytometry using a Cy3-labeled oligonucleotide. In this study, flow cytometry was used to rule out decreased association with the cell surface or decreased total cellular uptake as reasons for the decreased activity observed upon knockdown of COPII or STX5. Finally, and most critical for their conclusions, confocal fluorescence microscopy studies were used to examine co-localization of Cy3-labeled oligonucleotides and GFP-Rab7 or dye-labeled antibodies of endocytic markers. These co-localization experiments were conducted in untreated cells, cells treated with PS-oligonucleotide, and cells treated with PS-oligonucleotide and chloroquine to halt endosomal maturation.

This study strongly supports a role for COPII vesicles and STX5 in the endosomal escape of PS-oligonucleotides. Still, this study illustrates the limitations of assays currently used to measure uptake and intracellular trafficking. Key data on the trafficking of Cy3-labeled oligonucleotides were obtained by measuring co-localization using confocal fluorescence microscopy. After treatment with the RNA therapeutic, cells were fixed and permeabilized prior to staining with antibodies against specific endocytic markers. As several studies have shown (33,51,86,108,109), fixation can allow for redistribution of oligonucleotides and other biomolecules during subsequent incubation steps. When investigating subcellular localization, it is inherently problematic to interpret results from fixed and permeabilized cells. While these fluorescence co-localization experiments demonstrate association of PS-oligonucleotides with vesicles that also stain positive for COPII and STX5, they cannot distinguish material inside the late endosome from material bound to the exterior, or definitively show that material did not re-distribute following fixation and permeabilization. Despite these caveats, these assays are currently the best available for analysis of oligonucleotide trafficking through the endosomal pathway. This example highlights the need for additional assays that provide direct and quantitative insight into the subcellular trafficking of RNA therapeutics, with greater resolution with respect to cellular compartments and without steps that alter membrane structure such as fixation and permeabilization.

Together, these studies emphasize that many uptake assays must be conducted in parallel to fully understand a protein's role in the uptake and endosomal escape of RNA therapeutics. Implementing all of the available assays produces adequate results, but still has caveats and gaps in data interpretation. The field of RNA therapeutics would greatly benefit from the adoption of existing assays that can better quantitate subcellular localization, as well as from investment into assay development to design novel and improved assays to track subcellular localization.

CONCLUSION

The field of RNA therapeutics continues to deliver new therapies for otherwise intractable diseases. As a whole, the field has made impressive strides in developing chemical modifications and delivery strategies that increase *in vitro* and *in vivo* potency, yet efficient delivery to the cytosol/nucleus remains a major bottleneck. A great deal of time and resources are being directed toward improving tissue specificity, enhancing cellular uptake, and improving cytosolic/nuclear delivery. Despite these efforts, the efficacy of an RNA therapeutic *in vitro* does not always correlate with its *in vivo* efficacy. While a large number of factors may account for this discrepancy, it will be difficult to answer key questions without improving the methods used to analyze subcellular localization. Using a combination of existing and new methods, it will soon be possible to more definitively identify the key pathways and cellular factors for efficient cytosolic/nuclear penetration of RNA therapeutics.

FUNDING

USA National Institutes of Health (NIH) [GM127585]. Funding for open access charge: NIH [GM127585].
Conflict of interest statement. None declared.

REFERENCES

- Zamecnik, P.C. and Stephenson, M.L. (1978) Inhibition of Rous sarcoma virus replication and cell transformation by a specific oligodeoxynucleotide. *Proc. Natl. Acad. Sci. U.S.A.*, **75**, 280–284.
- Fire, A., Xu, S., Montgomery, M.K., Kostas, S.A., Driver, S.E. and Mello, C.C. (1998) Potent and specific genetic interference by double-stranded RNA in *Caenorhabditis elegans*. *Nature*, **391**, 806–811.
- Bennett, C.F. and Swayze, E.E. (2010) RNA targeting therapeutics: molecular mechanisms of antisense oligonucleotides as a therapeutic platform. *Annu. Rev. Pharmacol. Toxicol.*, **50**, 259–293.
- Crooke, S.T. (2017) Molecular mechanisms of antisense oligonucleotides. *Nucleic Acid Ther.*, **27**, 70–77.
- Hammond, S.M., Caudy, A.A. and Hannon, Gregory, J. (2001) Post-transcriptional gene silencing by double-stranded RNA. *Nat. Rev. Genet.*, **2**, 110–119.
- Catani, M., De Luca, C., Medeiros Garcia Alcántara, J., Manfredini, N., Perrone, D., Marchesi, E., Weldon, R., Müller-Spáth, T., Cavazzini, A., Morbidelli, M. *et al.* (2020) Oligonucleotides: current trends and innovative applications in the synthesis, characterization and purification. *Biotechnol. J.*, **16**, e1900226
- Dong, Y., Siegwart, D.J. and Anderson, D.G. (2019) Strategies, design and chemistry in siRNA delivery systems. *Adv. Drug Deliv. Rev.*, **144**, 133–147.
- Khvorova, A. and Watts, J.K. (2017) The chemical evolution of oligonucleotide therapies of clinical utility. *Nat. Biotechnol.*, **35**, 238–248.
- Wang, F., Zuroske, T. and Watts, J.K. (2020) RNA therapeutics on the rise. *Nat. Rev. Drug Discov.*, **19**, 441–442.
- Jabs, D.A. and Griffiths, P.D. (2002) Fomivirsen for the treatment of cytomegalovirus retinitis. *Am. J. Ophthalmol.*, **133**, 552–556.
- Hair, P., Cameron, F. and McKeage, K. (2013) Mipomersen sodium: first global approval. *Drugs*, **73**, 487–493.
- Corey, D.R. (2017) Nusinersen, an antisense oligonucleotide drug for spinal muscular atrophy. *Nat. Neurosci.*, **20**, 497–499.
- Lim, K., Maruyama, R. and Yokota, T. (2017) Eteplirsen in the treatment of Duchenne muscular dystrophy. *Drug Des. Devel. Ther.*, **11**, 533–545.
- Heo, Y.-A. (2020) Golodirsen: first approval. *Drugs*, **80**, 329–333.
- Keam, S.J. (2018) Inotersen: first global approval. *Drugs*, **78**, 1371–1376.
- Paik, J. and Duggan, S. (2019) Volanesorsen: first global approval. *Drugs*, **79**, 1349–1354.
- Shen, X. and Corey, D.R. (2018) Chemistry, mechanism and clinical status of antisense oligonucleotides and duplex RNAs. *Nucleic Acids Res.*, **46**, 1584–1600.
- Hoy, S.M. (2018) Patisiran: first global approval. *Drugs*, **78**, 1625–1631.
- Scott, L.J. (2020) Givosiran: first approval. *Drugs*, **80**, 335–339.
- Setten, R.L., Rossi, J.J. and Han, S. (2019) The current state and future directions of RNAi-based therapeutics. *Nat. Rev. Drug Discov.*, **18**, 421–446.
- Kim, J., Hu, C., Moufawad El Achkar, C., Black, L.E., Douville, J., Larson, A., Pendergast, M.K., Goldkind, S.F., Lee, E.A., Kuniholm, A. *et al.* (2019) Patient-customized oligonucleotide therapy for a rare genetic disease. *N. Engl. J. Med.*, **381**, 1644–1652.
- Philpott, J.R. and Miner, P.B. (2008) Antisense inhibition of ICAM-1 expression as therapy provides insight into basic inflammatory pathways through early experiences in IBD. *Expert Opin. Biol. Ther.*, **8**, 1627–1632.
- Mendell, J. (2017) Clinical trials of exon skipping in Duchenne muscular dystrophy. *Expert Opin. Orphan Drugs*, **5**, 683–690.
- Goemans, N., Mercuri, E., Belousova, E., Komaki, H., Dubrovsky, A., McDonald, C.M., Kraus, J.E., Loubbakos, A., Lin, Z., Campion, G. *et al.* (2018) A randomized placebo-controlled phase 3 trial of an antisense oligonucleotide, drisapersen, in Duchenne muscular dystrophy. *Neuromuscul. Disord.*, **28**, 4–15.
- Brad Wan, W. and Seth, P.P. (2016) The Medicinal Chemistry of Therapeutic Oligonucleotides. *J. Med. Chem.*, **59**, 9645–9667.
- Matsukura, M., Shinozuka, K., Zont, G., Mitsuya, H., Reitz, M., Cohent, J.S. and Broder, S. (1987) Phosphorothioate analogs of oligodeoxynucleotides: Inhibitors of replication and cytopathic effects of human immunodeficiency virus. *Proc. Natl. Acad. Sci. U.S.A.*, **84**, 7706–7710.
- Eckstein, F. (2014) Phosphorothioates, Essential Components of Therapeutic Oligonucleotides. *Nucleic Acid Ther.*, **24**, 374–387.
- Inoue, H., Hayase, Y., Hnura, A., Iwai, S., Miura, K. and Ohtsuka, E. (1987) Synthesis and hybridization studies on two complementary nona(2'-O-methyl)ribonucleotides. *Nucleic Acids Res.*, **15**, 6131–6148.
- Monia, B.P., Lesnik, E.A., Gonzalez, C., Lima, W.F., McGee, D., Guinasso, C.J., Kawasaki, A.M., Dan Cook, P. and Freier, S.M. (1993) Evaluation of 2'-modified oligonucleotides containing 2'-deoxy gaps as antisense inhibitors of gene expression. *J. Biol. Chem.*, **268**, 14514–14522.
- Manoharan, M. (1999) 2'-Carbohydrate modifications in antisense oligonucleotide therapy: Importance of conformation, configuration and conjugation. *Biochim. Biophys. Acta*, **1489**, 117–130.
- Koshkin, A.A., Singh, S.K., Nielsen, P., Rajwanshi, V.K., Kumar, R., Meldgaard, M., Olsen, C.E. and Wengel, J. (1998) LNA (Locked Nucleic Acid): synthesis of the adenine, cytosine, guanine, 5-methylcytosine, thymine and uracil bicyclonucleoside monomers, oligomerisation and unprecedented nucleic acid recognition. *Tetrahedron*, **54**, 3607–3630.
- Stanzl, E.G., Trantow, B.M., Vargas, J.R. and Wender, P.A. (2013) Fifteen years of cell-penetrating, guanidinium-rich molecular transporters: basic science, research tools and clinical applications. *Acc. Chem. Res.*, **46**, 2944–2954.
- Deglanc, G., Abes, S., Michel, T., Prévot, P., Vives, E., Debart, F., Barvik, I., Lebleu, B. and Vasseur, J.J. (2006) Impact of the guanidinium group on hybridization and cellular uptake of cationic oligonucleotides. *ChemBioChem*, **7**, 684–692.
- Stein, C.A., Hansen, J.B., Lai, J., Wu, S.J., Voskresenskiy, A., Høg, A., Worm, J., Hedtjärn, M., Souleimanian, N., Miller, P. *et al.* (2009) Efficient gene silencing by delivery of locked nucleic acid antisense oligonucleotides, unassisted by transfection reagents. *Nucleic Acids Res.*, **38**, e3.
- Juliano, R.L. (2016) The delivery of therapeutic oligonucleotides. *Nucleic Acids Res.*, **44**, 6518–6548.
- Bergan, R., Connell, Y., Fahmy, B. and Neckers, L. (1993) Electroporation enhances c-myc antisense oligodeoxynucleotide efficacy. *Nucleic Acids Res.*, **21**, 3567–3573.
- Fisher, T.L., Terhorst, T., Cao, X. and Wagner, R.W. (1993) Intracellular disposition and metabolism of fluorescently-labeled

- unmodified and modified oligonucleotides microinjected into mammalian cells. *Nucleic Acids Res.*, **21**, 3857–3865.
38. Chen,Z., Li,H., Zhang,L., Lee,C.K., Wai,L., Ho,C., Ka,C., Chan,W., Yang,H., Hang,C. *et al.* (2019) Specific delivery of oligonucleotides to the cell nucleus via gentle compression and attachment of polythymidine. *ACS Appl. Mater. Interfaces*, **11**, 27624–27640.
 39. Bennett,C.F., Chiang,M.Y., Chan,H., Shoemaker,J.E. and Mirabelli,C.K. (1992) Cationic lipids enhance cellular uptake and activity of phosphorothioate antisense oligonucleotides. *Mol. Pharmacol.*, **41**, 1023–1033.
 40. Wang,T., Larcher,L., Ma,L. and Veedu,R. (2018) Systematic screening of commonly used commercial transfection reagents towards efficient transfection of single-stranded oligonucleotides. *Molecules*, **23**, 2564.
 41. Litzinger,D.C. (1997) Limitations of cationic liposomes for antisense oligonucleotide delivery in vivo. *J. Liposome Res.*, **7**, 51–61.
 42. Prakash,T.P., Lima,W.F., Murray,H.M., Elbashir,S., Cantley,W., Foster,D., Jayaraman,M., Chappell,A.E., Manoharan,M., Swayze,E.E. *et al.* (2013) Lipid nanoparticles improve activity of single-stranded siRNA and gapmer antisense oligonucleotides in animals. *ACS Chem. Biol.*, **8**, 1402–1406.
 43. Osborn,M.F. and Khvorova,A. (2018) Improving siRNA delivery in vivo through lipid conjugation. *Nucleic Acid Ther.*, **28**, 128–136.
 44. Wang,S., Allen,N., Prakash,T.P., Liang,X. and Crooke,S.T. (2019) Lipid conjugates enhance endosomal release of antisense oligonucleotides into cells. *Nucleic Acid Ther.*, **29**, 245–255.
 45. Boisguérin,P., Deshayes,S., Gait,M.J., O'donovan,L., Godfrey,C., Betts,C.A., Wood,M.J.A. and Lebleu,B. (2015) Delivery of therapeutic oligonucleotides with cell penetrating peptides. *Adv. Drug Deliv. Rev.*, **87**, 52–67.
 46. Seth,P.P., Tanowitz,M. and Bennett,C.F. (2019) Selective tissue targeting of synthetic nucleic acid drugs. *J. Clin. Invest.*, **129**, 915–925.
 47. Prakash,T.P., Graham,M.J., Yu,J., Carty,R., Low,A., Chappell,A., Schmidt,K., Zhao,C., Aghajan,M., Murray,H.F. *et al.* (2014) Targeted delivery of antisense oligonucleotides to hepatocytes using triantennary N-acetyl galactosamine improves potency 10-fold in mice. *Nucleic Acids Res.*, **42**, 8796–8807.
 48. Geary,R.S., Wancewicz,E., Matson,J., Pearce,M., Siwkowski,A., Swayze,E. and Bennett,F. (2009) Effect of dose and plasma concentration on liver uptake and pharmacologic activity of a 2'-methoxyethyl modified chimeric antisense oligonucleotide targeting PTEN. *Biochem. Pharmacol.*, **78**, 284–291.
 49. Liang,X.H., Sun,H., Nichols,J.G. and Crooke,S.T. (2017) RNase H1-dependent antisense oligonucleotides are robustly active in directing RNA cleavage in both the cytoplasm and the nucleus. *Mol. Ther.*, **25**, 2075–2092.
 50. Pendergraft,H., Schmidt,S., Vikeså,J., Weile,C., Øverup,C., Lindholm,M.W. and Koch,T. (2020) Nuclear and cytoplasmic quantification of unconjugated, label-free locked nucleic acid oligonucleotides. *Nucleic Acid Ther.*, **30**, 4–13.
 51. González-Barriga,A., Nillessen,B., Kranzen,J., van Kessel,I.D.G., Croes,H.J.E., Aguilera,B., de Visser,P.C., Datson,N.A., Mulders,S.A.M., van Deutekom,J.C.T. *et al.* (2017) Intracellular distribution and nuclear activity of antisense oligonucleotides after unassisted uptake in myoblasts and differentiated myotubes in vitro. *Nucleic Acid Ther.*, **27**, 144–158.
 52. Heissig,P., Schrimpf,W., Hadwiger,P., Wagner,E. and Lamb,D.C. (2017) Monitoring integrity and localization of modified single-stranded RNA oligonucleotides using ultrasensitive fluorescence methods. *PLoS One*, **12**, e0173401.
 53. Buntz,A., Killian,T., Schmid,D., Seul,H., Brinkmann,U., Ravn,J., Lindholm,M., Knoetgen,H., Haucke,V. and Mundigl,O. (2019) Quantitative fluorescence imaging determines the absolute number of locked nucleic acid oligonucleotides needed for suppression of target gene expression. *Nucleic Acids Res.*, **47**, 953–969.
 54. Soares,R.J., Maglieri,G., Gutschner,T., Diederichs,S., Lund,A.H., Nielsen,B.S. and Holmstrøm,K. (2018) Evaluation of fluorescence in situ hybridization techniques to study long non-coding RNA expression in cultured cells. *Nucleic Acids Res.*, **46**, e4.
 55. Bailey,J.K., Shen,W., Liang,X. and Crooke,S.T. (2017) Nucleic acid binding proteins affect the subcellular distribution of phosphorothioate antisense oligonucleotides. *Nucleic Acids Res.*, **45**, 10649–10671.
 56. Querido,E., Dekakra-Bellili,L. and Chartrand,P. (2017) RNA fluorescence in situ hybridization for high-content screening. *Methods*, **126**, 149–155.
 57. Flanagan,W.M., Kothavale,A. and Wagner,R.W. (1996) Effects of oligonucleotide length, mismatches and mRNA levels on C-5 propyne-modified antisense potency. *Nucleic Acids Res.*, **24**, 2936–2941.
 58. Witttrup,A., Ai,A., Liu,X., Hamar,P., Trifonova,R., Charisse,K., Manoharan,M., Kirchhausen,T. and Lieberman,J. (2015) Visualizing lipid-formulated siRNA release from endosomes and target gene knockdown. *Nat. Biotechnol.*, **33**, 870–876.
 59. Yang,L., Ma,F., Liu,F., Chen,J., Zhao,X. and Xu,Q. (2020) Efficient delivery of antisense oligonucleotides using bioreducible lipid nanoparticles in vitro and in vivo. *Mol. Ther. - Nucleic Acids*, **19**, 1357–1367.
 60. Deleavey,G.F., Watts,J.K., Alain,T., Robert,F., Kalota,A., Aishwarya,V., Pelletier,J., Gewirtz,A.M., Sonenberg,N. and Damha,M.J. (2010) Synergistic effects between analogs of DNA and RNA improve the potency of siRNA-mediated gene silencing. *Nucleic Acids Res.*, **38**, 4547–4557.
 61. Kang,S.-H., Cho,M.-J. and Kole,R. (1998) Up-regulation of luciferase gene expression with antisense oligonucleotides: implications and applications in functional assay development. *Biochemistry*, **37**, 6235–6239.
 62. Sazani,P., Kang,S.-H., Maier,M.A., Wei,C., Dillman,J., Summerton,J., Manoharan,M. and Kole,R. (2001) Nuclear antisense effects of neutral, anionic and cationic oligonucleotide analogs. *Nucleic Acids Res.*, **29**, 3965–3974.
 63. Jiang,Z., Zheng,X. and Rich,K.M. (2003) Down-regulation of Bcl-2 and Bcl-xL expression with bispecific antisense treatment in glioblastoma cell lines induce cell death. *J. Neurochem.*, **84**, 273–281.
 64. Janas,M.M., Jiang,Y., Schlegel,M.K., Waldron,S., Kuchimanchi,S. and Barros,S.A. (2017) Impact of oligonucleotide structure, chemistry and delivery method on in vitro cytotoxicity. *Nucleic Acid Ther.*, **27**, 11–22.
 65. Stanton,R., Sciabola,S., Salatto,C., Weng,Y., Moshinsky,D., Little,J., Walters,E., Kreeger,J., Dimattia,D., Chen,T. *et al.* (2012) Chemical modification study of antisense gapmers. *Nucleic Acid Ther.*, **22**, 344–359.
 66. Drygin,D., Barone,S. and Bennett,C.F. (2004) Sequence-dependent cytotoxicity of second-generation oligonucleotides. *Nucleic Acids Res.*, **32**, 6585–6594.
 67. Gagnon,K.T. and Corey,D.R. (2019) Guidelines for experiments using antisense oligonucleotides and double-stranded RNAs. *Nucleic Acid Ther.*, **29**, 116–122.
 68. Huber-Ruano,I., Raventós,C., Cuartas,I., Sánchez-Jaro,C., Arias,A., Parra,J.L., Wosikowski,K., Janicot,M. and Seoane,J. (2017) An antisense oligonucleotide targeting TGF- β 2 inhibits lung metastasis and induces CD86 expression in tumor-associated macrophages. *Ann. Oncol.*, **28**, 2278–2285.
 69. Crooke,S.T., Wang,S., Vickers,T.A., Shen,W. and Liang,X. (2017) Cellular uptake and trafficking of antisense oligonucleotides. *Nat. Biotechnol.*, **35**, 230–237.
 70. Deprey,K., Becker,L., Kritzer,J. and Plückthun,A. (2019) Trapped! A critical evaluation of methods for measuring total cellular uptake versus cytosolic localization. *Bioconjug. Chem.*, **30**, 1006–1027.
 71. Méndez Ardoy,A., Lostalé-Seijo,I. and Montenegro,J. (2019) Where in the cell is our cargo? Current methods to study intracellular cytosolic localization. *ChemBioChem*, **20**, 488–498.
 72. Iversen,P.L., Zhu,S., Meyer,A. and Zon,G. (1992) Cellular uptake and subcellular distribution of phosphorothioate oligonucleotides into cultured cells. *Antisense Res. Dev.*, **2**, 211–222.
 73. Beltinger,C., Saragovi,H.U., Smith,R.M., LeSauter,L., Shah,N., DeDionisio,L., Christensen,L., Raible,A., Jarett,L. and Gewirtz,A.M. (1995) Binding, uptake and intracellular trafficking of phosphorothioate-modified oligodeoxynucleotides. *J. Clin. Invest.*, **95**, 1814–1823.
 74. Agrawal,S., Tamsamani,J. and Tang,J.Y. (1991) Pharmacokinetics, biodistribution and stability of oligodeoxynucleotide phosphorothioates in mice. *Proc. Natl. Acad. Sci. U.S.A.*, **88**, 7595–7599.

75. Bijsterbosch, M.K., Manoharan, M., Rump, E.T., De Vruet, R.L.A., Van Veghel, R., Tivel, K.L., Biessen, E.A.L., Bennett, C.F., Cook, P.D. and Van Berkel, T.J.C. (1997) In vivo fate of phosphorothioate antisense oligodeoxynucleotides: predominant uptake by scavenger receptors on endothelial liver cells. *Nucleic Acids Res.*, **25**, 3290–3296.
76. Christensen, J., Litherland, K., Faller, T., Van De Kerkhof, E., Natt, F., Hunziker, J., Krauser, J., Swart, P. and Center, B. (2013) Metabolism studies of unformulated internally [³H]-labeled short interfering RNAs in mice. *Drug Metab. Dispos.*, **41**, 1211–1219.
77. Ballal, R., Cheema, A., Ahmad, W., Rosen, E.M. and Saha, T. (2009) Fluorescent oligonucleotides can serve as suitable alternatives to radiolabeled oligonucleotides. *J. Biomol. Tech.*, **20**, 190–194.
78. Zhao, Q., Zhou, R., Temsamani, J., Zhang, Z., Roskey, A. and Agrawal, S. (1998) Cellular distribution of phosphorothioate oligonucleotide following intravenous administration in mice. *Antisense Nucleic Acid Drug Dev.*, **8**, 451–458.
79. Tanowitz, M., Hettrick, L., Revenko, A., Kinberger, G.A., Prakash, T.P. and Seth, P.P. (2017) Asialoglycoprotein receptor 1 mediates productive uptake of N-acetylgalactosamine-conjugated and unconjugated phosphorothioate antisense oligonucleotides into liver hepatocytes. *Nucleic Acids Res.*, **45**, 12388–12400.
80. Liang, X.-H., Sun, H., Nichols, J.G., Allen, N., Wang, S., Vickers, T.A., Shen, W., Hsu, C.-W. and Crooke, S.T. (2018) COPII vesicles can affect the activity of antisense oligonucleotides by facilitating the release of oligonucleotides from endocytic pathways. *Nucleic Acids Res.*, **46**, 10225–10245.
81. Sharma, V.K., Osborn, M.F., Hassler, M.R., Echeverria, D., Ly, S., Ulashchik, E.A., Yury, I., Martynenko-Makaev, V., Shmanai, V. V., Zatselin, T.S. *et al.* (2018) Novel cluster and monomer-based GalNAc structures induce effective uptake of siRNAs in vitro and in vivo. *Bioconjug. Chem.*, **29**, 2478–2488.
82. Juliano, R.L., Wang, L., Tavares, F., Brown, E.G., James, L., Ariyaratna, Y., Ming, X., Mao, C. and Suto, M. (2018) Structure–activity relationships and cellular mechanism of action of small molecules that enhance the delivery of oligonucleotides. *Nucleic Acids Res.*, **46**, 1601–1613.
83. Puckett, C.A. and Barton, J.K. (2009) Fluorescein redirects a ruthenium-octaarginine conjugate to the nucleus. *J. Am. Chem. Soc.*, **131**, 8738–8739.
84. Birch, D., Christensen, M.V., Staerk, D., Franzky, H. and Nielsen, H.M. (2017) Fluorophore labeling of a cell-penetrating peptide induces differential effects on its cellular distribution and affects cell viability. *Biochim. Biophys. Acta - Biomembr.* **1859**, 2483–2494.
85. Hedegaard, S.F., Derbas, M.S., Lind, T.K., Kasimova, M.R., Christensen, M.V., Michaelsen, M.H., Campbell, R.A., Jorgensen, L., Franzky, H., Cárdenas, M. *et al.* (2018) Fluorophore labeling of a cell-penetrating peptide significantly alters the mode and degree of biomembrane interaction. *Sci. Rep.*, **8**, 6327.
86. Lacroix, A., Vengut-Climent, E., De Rochambeau, D. and Sleiman, H.F. (2019) Uptake and fate of fluorescently labeled DNA nanostructures in cellular environments: a cautionary tale. *ACS Cent. Sci.*, **5**, 882–891.
87. Praus, P., Kocisova, E., Seksek, O., Sureau, F., Stepanek, J. and Turpin, P.-Y. (2007) Advanced microfluorescence methods in monitoring intracellular uptake of “Antisense” oligonucleotides. *Curr. Org. Chem.*, **11**, 515–527.
88. De Smedt, S.C., Remaut, K., Lucas, B., Braeckmans, K., Sanders, N.N. and Demeester, J. (2005) Studying biophysical barriers to DNA delivery by advanced light microscopy. *Adv. Drug Deliv. Rev.*, **57**, 191–210.
89. Praus, P., Kočíšová, E., Moješ, P., Štěpánek, J., Seksek, O., Sureau, F. and Turpin, P.-Y. (2008) Time-resolved microspectrofluorometry and fluorescence imaging techniques: study of porphyrin-mediated cellular uptake of oligonucleotides. *Ann. N. Y. Acad. Sci.*, **1130**, 117–121.
90. Praus, P., Kočíšová, E., Moješ, P., Štěpánek, J., Turpin, P.Y. and Sureau, F. (2011) Cellular uptake of modified oligonucleotides enhanced by porphyrins studied by time-resolved microspectrofluorimetry and fluorescence imaging techniques. *J. Mol. Struct.*, **993**, 316–318.
91. Leontien Van Der Bent, M., Wansink, D.G. and Brock, R. (2020) Advanced fluorescence imaging to distinguish between intracellular fractions of antisense oligonucleotides. *Methods Mol. Biol.*, **2063**, 119–138.
92. Knemeyer, J.P., Herten, D.P. and Sauer, M. (2003) Detection and identification of single molecules in living cells using spectrally resolved fluorescence lifetime imaging microscopy. *Anal. Chem.*, **75**, 2147–2153.
93. Leontien Van Der Bent, M., Paulino Da, O., Filho, S., Willemse, M., Hällbrink, M., Wansink, D.G. and Brock, R. (2019) The nuclear concentration required for antisense oligonucleotide activity in myotonic dystrophy cells. *FASEB J.*, **33**, 11314–11325.
94. Luo, T., Zhou, T., Zhao, Y., Liu, L. and Qu, J. (2018) Multiplexed fluorescence lifetime imaging by concentration-dependent quenching. *J. Mater. Chem. B*, **6**, 1912–1919.
95. Damalakiene, L., Karabanovas, V., Bagdonas, S., Rotomskis, R. and Sivakov, V. (2016) Fluorescence-lifetime imaging microscopy for visualization of quantum dots’ endocytic pathway. *Int. J. Mol. Sci.*, **17**, 473.
96. Reyderman, L. and Stavchansky, S. (1996) Determination of single-stranded oligodeoxynucleotides by capillary gel electrophoresis with laser induced fluorescence and on column derivatization. *J. Chromatogr. A*, **755**, 271–280.
97. Kolesar, J.M., Allen, P.G. and Doran, C.M. (1997) Direct quantification of HIV-1 RNA by capillary electrophoresis with laser-induced fluorescence. *J. Chromatogr. B*, **697**, 189–194.
98. Goldsmith, J.G., Ntuen, E.C. and Goldsmith, E.C. (2007) Direct quantification of gene expression using capillary electrophoresis with laser-induced fluorescence. *Anal. Biochem.*, **360**, 23–29.
99. Al-Mahrouki, A.A. and Krylov, S.N. (2005) Calibration-free quantitative analysis of mRNA. *Anal. Chem.*, **77**, 8027–8030.
100. McKeon, J., Cho, M.J. and Khaledi, M.G. (2001) Quantitation of intracellular concentration of a delivered morpholino oligomer by capillary electrophoresis-laser-induced fluorescence: Correlation with upregulation of luciferase gene expression. *Anal. Biochem.*, **293**, 1–7.
101. McKeon, J. and Khaledi, M.G. (2001) Quantitative nuclear and cytoplasmic localization of antisense oligonucleotides by capillary electrophoresis with laser-induced fluorescence detection. *Electrophoresis*, **22**, 3765–3770.
102. McKeon, J. and Khaledi, M.G. (2003) Evaluation of liposomal delivery of antisense oligonucleotide by capillary electrophoresis with laser-induced fluorescence detection. *J. Chromatogr. A*, **1004**, 39–46.
103. Malek, A.H. and Khaledi, M.G. (2003) Monitoring liposome-mediated delivery and fate of an antisense drug in cell extracts and in single cells by capillary electrophoresis with laser-induced fluorescence. *Electrophoresis*, **24**, 1054–1062.
104. Oehlke, J., Birth, P., Klauschen, E., Wiesner, B., Beyermann, M., Oksche, A. and Bienert, M. (2002) Cellular uptake of antisense oligonucleotides after complexing or conjugation with cell-penetrating model peptides. *Eur. J. Biochem.*, **269**, 4025–4032.
105. Koller, E., Vincent, T.M., Chappell, A., De, S., Manoharan, M. and Bennett, C.F. (2011) Mechanisms of single-stranded phosphorothioate modified antisense oligonucleotide accumulation in hepatocytes. *Nucleic Acids Res.*, **39**, 4795–4807.
106. Ponnath, A., Depreux, F.F., Jodelka, F.M., Rigo, F., Farris, H.E., Hastings, M.L. and Lentz, J.J. (2018) Rescue of outer hair cells with antisense oligonucleotides in Usher mice is dependent on age of treatment. *J. Assoc. Res. Otolaryngol.*, **9**, 1–16.
107. Linnane, E., Davey, P., Zhang, P., Puri, S., Edbrooke, M., Chiarparin, E., Revenko, A.S., Robert Macleod, A., Norman, J.C. and Ross, S.J. (2019) Differential uptake, kinetics and mechanisms of intracellular trafficking of next-generation antisense oligonucleotides across human cancer cell lines. *Nucleic Acids Res.*, **47**, 4375–4392.
108. Pichon, C., Monsigny, M. and Roche, A.C. (1999) Intracellular localization of oligonucleotides: influence of fixative protocols. *Antisense Nucleic Acid Drug Dev.*, **9**, 89–93.
109. Belitsky, J.M., Leslie, S.J., Arora, P.S., Beerman, T.A. and Dervan, P.B. (2002) Cellular uptake of N-methylpyrrole/N-methylimidazole polyamide-dye conjugates. *Bioorganic Med. Chem.*, **10**, 3313–3318.
110. Krafčikova, M., Dzatko, S., Caron, C., Granzhan, A., Fiala, R., Loja, T., Teulade-Fichou, M.P., Fessl, T., Hänsel-Hertsch, R., Mergny, J.L. *et al.* (2019) Monitoring DNA-ligand interactions in living human cells using NMR spectroscopy. *J. Am. Chem. Soc.*, **141**, 13281–13285.

111. Hänsel, R., Foldynová-Trantírková, S., Löhr, F., Buck, J., Bongartz, E., Bamberg, E., Schwalbe, H., Dötsch, V. and Trantírek, L. (2009) Evaluation of parameters critical for observing nucleic acids inside living *Xenopus laevis* oocytes by in-cell NMR spectroscopy. *J. Am. Chem. Soc.*, **131**, 15761–15768.
112. Dzatko, S., Krafčíková, M., Hänsel-Hertsch, R., Fessl, T., Fiala, R., Loja, T., Krafčík, D., Mergny, J.-L., Foldynová-Trantírková, S. and Trantírek, L. (2018) Evaluation of the stability of DNA i-motifs in the nuclei of living mammalian cells. *Angew. Chem. Int. Ed.*, **57**, 2165–2169.
113. Yamaoki, Y., Kiyoshi, A., Miyake, M., Kano, F., Murata, M., Nagata, T. and Katahira, M. (2018) The first successful observation of in-cell NMR signals of DNA and RNA in living human cells. *Phys. Chem. Chem. Phys.*, **20**, 2982–2985.
114. Viskova, P., Krafčík, D., Trantírek, L. and Foldynová-Trantírková, S. (2019) In-cell NMR spectroscopy of nucleic acids in human cells. *Curr. Protoc. Nucleic Acid Chem.*, **76**, e71.
115. Schlagnitweit, J., Friebe Sandoz, S., Jaworski, A., Guzzetti, I., Aussenac, F., Carbajo, R. J., Chiarparrin, E., Pell, A. J. and Petzold, K. (2019) Observing an antisense drug complex in intact human cells by in-cell NMR spectroscopy. *ChemBioChem*, **20**, 2474–2478.
116. Studzińska, S. (2018) Review on investigations of antisense oligonucleotides with the use of mass spectrometry. *Talanta*, **176**, 329–343.
117. Studzińska, S., Cywoniuk, P. and Sobczak, K. (2019) Application of ion pair chromatography coupled with mass spectrometry to assess antisense oligonucleotides concentrations in living cells †. *Analyst*, **144**, 622–633.
118. Liu, J., Li, J., Tran, C., Aluri, K., Zhang, X., Clausen, V., Zlatev, I., Guan, L., Chong, S., Charisse, K. et al. (2019) Oligonucleotide quantification and metabolite profiling by high-resolution and accurate mass spectrometry. *Bioanalysis*, **11**, 1967–1980.
119. Ramanathan, L. and Shen, H. (2019) LC-TOF-MS methods to quantify siRNAs and major metabolite in plasma, urine and tissues. *Bioanalysis*, **11**, 1983–1992.
120. Straarup, E. M., Fisker, N., Lindholm, M. W., Rosenbohm, C., Aarup, V., Hansen, H. F., Ørum, H., Hansen, J. B. R. and Koch, T. (2010) Short locked nucleic acid antisense oligonucleotides potentially reduce apolipoprotein B mRNA and serum cholesterol in mice and non-human primates. *Nucleic Acids Res.*, **38**, 7100–7111.
121. Yu, R. Z., Baker, B., Chappell, A., Geary, R. S., Cheung, E. and Levin, A. A. (2002) Development of an ultrasensitive noncompetitive hybridization-ligation enzyme-linked immunosorbent assay for the determination of phosphorothioate oligodeoxynucleotide in plasma. *Anal. Biochem.*, **304**, 19–25.
122. Wei, X., Dai, G., Marcucci, G., Liu, Z., Hoyt, D., Blum, W. and Chan, K. K. (2006) A specific picomolar hybridization-based ELISA assay for the determination of phosphorothioate oligonucleotides in plasma and cellular matrices. *Pharm. Res.*, **23**, 1251–1264.
123. Alachkar, H., Xie, Z., Marcucci, G. and Chan, K. K. (2012) Determination of cellular uptake and intracellular levels of Cenersen (Aezee®), EL625), a p53 antisense oligonucleotide in acute myeloid leukemia cells. *J. Pharm. Biomed. Anal.*, **71**, 228–232.
124. Melo, D., Maruyama, R. and Yokota, T. (2018) Systemic injection of peptide-PMOs into humanized DMD mice and evaluation by RT-PCR and ELISA. *Methods Mol. Biol.* **1828**, 263–273.
125. Burki, U., Keane, J., Blain, A., O'donovan, L., Gait, M. J., Laval, S. H. and Straub, V. (2015) Development and application of an ultrasensitive hybridization-based ELISA method for the determination of peptide-conjugated phosphorodiamidate morpholino oligonucleotides. *Nucleic Acid Ther.*, **25**, 275–284.
126. Hagedorn, P. H., Persson, R., Funder, E. D., Albæk, N., Diemer, S. L., Hansen, D. J., Møller, M. R., Papargyri, N., Christiansen, H., Hansen, B. R. et al. (2018) Locked nucleic acid: modality, diversity and drug discovery. *Drug Discov. Today*, **23**, 101–114.
127. Burki, U. and Straub, V. (2017) Ultrasensitive hybridization-based ELISA method for the determination of phosphorodiamidate morpholino oligonucleotides in biological samples. *Methods Mol. Biol.*, **1565**, 265–277.
128. Roehl, I., Schuster, M. and Seiffert, S. (2011) In: *Oligonucleotide Detection Method*.
129. Godinho, B. M. D. C., Gilbert, J. W., Haraszti, R. A., Coles, A. H., Biscans, A., Roux, L., Nikan, M., Echeverria, D., Hassler, M. and Khvorova, A. (2017) Pharmacokinetic profiling of conjugated therapeutic oligonucleotides: a high-throughput method based upon serial blood microsampling coupled to peptide nucleic acid hybridization assay. *Nucleic Acid Ther.*, **27**, 323–334.
130. Hassler, M. R., Turanov, A. A., Alterman, J. F., Haraszti, R. A., Coles, A. H., Osborn, M. F., Echeverria, D., Nikan, M., Salomon, W. E., Roux, L. L. et al. (2018) Comparison of partially and fully chemically-modified siRNA in conjugate-mediated delivery in vivo. *Nucleic Acids Res.*, **46**, 2185–2196.
131. Biscans, A., Coles, A., Echeverria, D. and Khvorova, A. (2019) The valency of fatty acid conjugates impacts siRNA pharmacokinetics, distribution and efficacy in vivo. *J. Control. Release*, **302**, 116–125.
132. Nikan, M., Osborn, M. F., Coles, A. H., Godinho, B. M., Hall, L. M., Haraszti, R. A., Hassler, M. R., Echeverria, D., Aronin, N. and Khvorova, A. (2016) Docosahexaenoic acid conjugation enhances distribution and safety of siRNA upon local administration in mouse brain. *Mol. Ther. - Nucleic Acids*, **5**, e344.
133. Haraszti, R. A., Roux, L., Coles, A. H., Turanov, A. A., Alterman, J. F., Echeverria, D., Godinho, B. M. D. C., Aronin, N. and Khvorova, A. (2017) 5-Vinylphosphonate improves tissue accumulation and efficacy of conjugated siRNAs in vivo. *Nucleic Acids Res.*, **45**, 7581–7592.
134. Biscans, A., Coles, A., Haraszti, R., Echeverria, D., Hassler, M., Osborn, M. and Khvorova, A. (2019) Diverse lipid conjugates for functional extra-hepatic siRNA delivery in vivo. *Nucleic Acids Res.*, **47**, 1082–1096.
135. Ji, Y., Liu, Y., Xia, W., Behling, A., Meng, M., Bennett, P. and Wang, L. (2019) Importance of probe design for bioanalysis of oligonucleotides using hybridization-based LC-fluorescence assays. *Bioanalysis*, **11**, 1917–1925.
136. Yoo, H. and Juliano, R. L. (2000) Enhanced delivery of antisense oligonucleotides with fluorophore-conjugated PAMAM dendrimers. *Nucleic Acids Res.*, **28**, 4225–4231.
137. Pasquali, C., Fialka, I. and Huber, L. A. (1999) Subcellular fractionation, electromigration analysis and mapping of organelles. *J. Chromatogr. B*, **722**, 89–102.
138. Vámosi, G., Damjanovich, S., Szöllösi, J. and Vereb, G. (2009) Measurement of molecular mobility with fluorescence correlation spectroscopy. *Curr. Protoc. Cytom.*, **50**, doi:10.1002/0471142956.cy0215s50.
139. Schwille, P. and Hausteiner, E. (2001) In: *Fluorescence Correlation Spectroscopy: An Introduction to its Concepts and Applications*. Germany.
140. Quach, K., LaRochelle, J., Li, X. H., Rhoades, E. and Schepartz, A. (2018) Unique arginine array improves cytosolic localization of hydrocarbon-stapled peptides. *Bioorganic Med. Chem.*, **26**, 1197–1202.
141. Schwille, P., Meyer-Almes, F.-J. and Rigler, R. (1997) Dual-color fluorescence cross-correlation spectroscopy for multicomponent diffusional analysis in solution. *Biophys. J.*, **72**, 1878–1886.
142. Ohrt, T., Rg Mü Tze, J., Staroske, W., Weinmann, L., Hö Ck, J., Crell, K., Meister, G. and Schwille, P. (2008) Fluorescence correlation spectroscopy and fluorescence cross-correlation spectroscopy reveal the cytoplasmic origination of loaded nuclear RISC in vivo in human cells. *Nucleic Acids Res.*, **36**, 6439–6449.
143. LaRochelle, J. R., Cobb, G. B., Steinauer, A., Rhoades, E. and Schepartz, A. (2015) Fluorescence correlation spectroscopy reveals highly efficient cytosolic delivery of certain penta-arg proteins and stapled peptides. *J. Am. Chem. Soc.*, **137**, 2536–2541.
144. Gilleron, J., Querbes, W., Zeigerer, A., Borodovsky, A., Marsico, G., Schubert, U., Manyoats, K., Seifert, S., Andree, C., St. M. et al. (2013) Image-based analysis of lipid nanoparticle-mediated siRNA delivery, intracellular trafficking and endosomal escape. *Nat. Biotechnol.*, **31**, 638–646.
145. Cabantous, S., Terwilliger, T. C. and Waldo, G. S. (2005) Protein tagging and detection with engineered self-assembling fragments of green fluorescent protein. *Nat. Biotechnol.*, **23**, 102–107.
146. Kato, N. and Jones, J. (2010) The split luciferase complementation assay. *Methods Mol. Biol.*, **655**, 359–376.
147. Milech, N., Longville, B. A., Cunningham, P. T., Scobie, M. N., Bogdawa, H. M., Winslow, S., Anastasas, M., Connor, T., Ong, F., Stone, S. R. et al. (2015) GFP-complementation assay to detect functional CPP and protein delivery into living cells. *Sci. Rep.*, **5**, 18329.

148. Yu, P., Liu, B. and Kodadek, T. (2005) A high-throughput assay for assessing the cell permeability of combinatorial libraries. *Nat. Biotechnol.*, **23**, 746–751.
149. Holub, J.M., Larochelle, J.R., Appelbaum, J.S. and Schepartz, A. (2013) Improved assays for determining the cytosolic access of peptides, proteins and their mimetics. *Biochemistry*, **52**, 9036–9046.
150. Verdurmen, W.P.R., Luginbühl, M., Honegger, A. and Plückthun, A. (2015) Efficient cell-specific uptake of binding proteins into the cytoplasm through engineered modular transport systems. *J. Control. Release*, **200**, 13–22.
151. Chyan, W. and Raines, R.T. (2018) Enzyme-activated fluorogenic probes for live-cell and in vivo imaging HHS public access. *ACS Chem. Biol.*, **13**, 1810–1823.
152. Peraro, L., Zou, Z., Makwana, K.M., Cummings, A.E., Ball, H.L., Yu, H., Lin, Y.S., Levine, B. and Kritzer, J.A. (2017) Diversity-oriented stapling yields intrinsically cell-penetrant inducers of autophagy. *J. Am. Chem. Soc.*, **139**, 7792–7802.
153. Peraro, L., Deprey, K.L., Moser, M.K., Zou, Z., Ball, H.L., Levine, B. and Kritzer, J.A. (2018) Cell penetration profiling using the chloroalkane penetration assay. *J. Am. Chem. Soc.*, **140**, 11360–11369.
154. Deprey, K. and Kritzer, J.A. (2020) Quantitative measurement of cytosolic penetration using the chloroalkane penetration assay. *Methods Enzymol.*, doi:10.1016/bs.mie.2020.03.003.
155. Ballister, E.R., Aonbangkhen, C., Mayo, A.M., Lampton, M.A. and Chenoweth, D.M. (2014) Localized light-induced protein dimerization in living cells using a photocaged dimerizer. *Nat. Commun.*, **5**, 5475.
156. Cai, B., Kim, D., Akhand, S., Sun, Y., Cassell, R.J., Alpsoy, A., Dykhuizen, E.C., Van Rijn, R.M., Wendt, M.K. and Krusemark, C.J. (2019) Selection of DNA-encoded libraries to protein targets within and on living cells. *J. Am. Chem. Soc.*, **141**, 17057–17061.
157. Foley, C.A., Potjeyd, F., Lamb, K.N., James, L.I. and Frye, S.V. (2020) Assessing the cell permeability of bivalent chemical degraders using the chloroalkane penetration assay. *ACS Chem. Biol.*, **15**, 290–295.
158. Lamb, K.N., Bsteh, D., Dishman, S.N., Moussa, H.F., Fan, H., Stuckey, J.I., Norris, J.L., Cholensky, S.H., Li, D., Wang, J. et al. (2019) Discovery and characterization of a cellular potent positive allosteric modulator of the polycomb repressive complex 1 chromodomain, CBX7. *Cell Chem. Biol.*, **26**, 1365–1379.
159. Shin, M.-K., Hyun, Y.-J., Lee, J.H. and Lim, H.-S. (2018) Comparison of cell permeability of cyclic peptoids and linear peptoids. *ACS Comb. Sci.*, **20**, 237–242.
160. Lopez-Andarias, J., Saabach, J., Moreau, D., Cheng, Y., Derivery, E., Laurent, Q., Gonzalez-Gaita, M., Winssinger, N., Sakai, N. and Matile, S. (2020) Cell-penetrating streptavidin: a general tool for bifunctional delivery with spatiotemporal control, mediated by transport systems such as adaptive benzopolysulfane networks. *J. Am. Chem. Soc.*, **142**, 4784–4792.
161. Yin, H., Huang, Y.-H., Deprey, K., Condon, N.D., Kritzer, J.A., Craik, D.J. and Wang, C.K. (2020) Cellular uptake and cytosolic delivery of a cyclic cystine knot scaffold. *ACS Chem. Biol.*, **15**, 1650–1661.
162. Soifer, H.S., Koch, T., Lai, J., Hansen, B., Hoeg, A., Oerum, H. and Stein, C.A. (2012) Silencing of gene expression by gymnotic delivery of antisense oligonucleotides. *Methods Mol. Biol.*, **815**, 333–346.
163. Juliano, R.L. (2018) Intracellular trafficking and endosomal release of oligonucleotides: what we know and what we don't. *Nucleic Acid Ther.*, **28**, 166–177.
164. Juliano, R.L., Carver, K., Cao, C. and Ming, X. (2013) Receptors, endocytosis and trafficking: the biological basis of targeted delivery of antisense and siRNA oligonucleotides. *J. Drug Target.*, **21**, 27–43.
165. Juliano, R.L., Ming, X., Carver, K. and Laing, B. (2014) Cellular uptake and intracellular trafficking of oligonucleotides: implications for oligonucleotide pharmacology. *Nucleic Acid Ther.*, **24**, 101–113.
166. Wang, S., Sun, H., Tanowitz, M., Liang, X.H. and Crooke, S.T. (2016) Annexin A2 facilitates endocytic trafficking of antisense oligonucleotides. *Nucleic Acids Res.*, **44**, 7314–7330.
167. Wang, S., Sun, H., Tanowitz, M., Liang, X.H. and Crooke, S.T. (2017) Intra-endosomal trafficking mediated by lysobisphosphatidic acid contributes to intracellular release of phosphorothioate-modified antisense oligonucleotides. *Nucleic Acids Res.*, **45**, 5309–5322.
168. Takahashi, M., Contu, V.R., Kabuta, C., Hase, K., Fujiwara, Y., Wada, K. and Kabuta, T. (2017) SIDT2 mediates gymnosis, the uptake of naked single-stranded oligonucleotides into living cells. *RNA Biol.*, **14**, 1534–1543.
169. Miller, C.M., Donner, A.J., Blank, E.E., Egger, A.W., Kellar, B.M., Østergaard, M.E., Seth, P.P. and Harris, E.N. (2016) Stabilin-1 and Stabilin-2 are specific receptors for the cellular internalization of phosphorothioate-modified antisense oligonucleotides (ASOs) in the liver. *Nucleic Acids Res.*, **44**, 2782–2794.
170. Wang, S., Allen, N., Vickers, T.A., Revenko, A.S., Sun, H., Liang, X. and Crooke, S.T. (2018) Cellular uptake mediated by epidermal growth factor receptor facilitates the intracellular activity of phosphorothioate-modified antisense oligonucleotides. *Nucleic Acids Res.*, **46**, 3579–3594.
171. Wiewer, M., Maritzen, T. and Haucke, V. (2009) SnapShot: endocytic trafficking. *Cell*, **137**, 382.
172. Schmid, E.M. and McMahon, H.T. (2007) Integrating molecular and network biology to decode endocytosis. *Nature*, **448**, 883–888.
173. Galli, V., Sadhu, K.K., Masi, D., Saabach, J., Roux, A. and Winssinger, N. (2020) Caprin-1 promotes cellular uptake of nucleic acids with backbone and sequence discrimination. *Helv. Chim. Acta*, **103**, e1900255.
174. Castanotto, D., Lin, M., Kowolik, C., Koch, T., Hansen, B.R., Oerum, H. and Stein, C.A. (2016) Protein kinase C- α is a critical protein for antisense oligonucleotide-mediated silencing in mammalian cells. *Mol. Ther.*, **24**, 1117–1125.
175. Wagenaar, T.R., Tolstykh, T., Shi, C., Jiang, L., Zhang, J., Li, Z., Yu, Q., Qu, H., Sun, F., Cao, H. et al. (2014) Identification of the endosomal sorting complex required for transport-I (ESCRT-I) as an important modulator of anti-miR uptake by cancer cells. *Nucleic Acids Res.*, **43**, 1204–1215.
176. Liang, X.-H., Sun, H., Hsu, C.-W., Nichols, J.G., Vickers, T.A., De Hoyos, C.L. and Crooke, S.T. (2020) Golgi-endosome transport mediated by M6PR facilitates release of antisense oligonucleotides from endosomes. *Nucleic Acids Res.*, **48**, 1372–1391.
177. Miller, C.M., Wan, W.B., Seth, P.P. and Harris, E.N. (2018) Endosomal escape of antisense oligonucleotides internalized by stabilin receptors is regulated by Rab5C and EEA1 during endosomal maturation. *Nucleic Acid Ther.*, **28**, 86–96.